(4)

AD-A222 085

SEVENTH QUARTERLY REPORT

FOR THE PROJECT

"COMPOSITE CERAMIC SUPERCONDUCTING WIRES FOR ELECTRIC MOTOR APPLICATIONS"

PRIME CONTRACTOR

CERAMICS PROCESS SYSTEMS CORPORATION
155 FORTUNE BOULEVARD
MILFORD, MASSACHUSETTS 01757

30 APRIL 1990

CPS 90-010

DARPA ORDER NO: 9525
CONTRACT NO: N00014-88-C-0512
CONTRACT EFFECTIVE DATE: 30 JUNE 1988
CONTRACT EXPIRATION DATE: 31 MARCH 1991
PRINCIPAL INVESTIGATOR: JOHN W. HALLORAN
(508) 634-3422

Prepared for
DEFENSE ADVANCED RESEARCH PROJECTS AGENCY
1400 Wilson Boulevard
Arlington, VA 22209

OFFICE OF NAVAL RESEARCH
800 North Quincy Street
Arlington, VA 22217-5000

APPROVED FOR PUBLIC RELEASE: DISTRIBUTION IS UNLIMITED

REPORT DOCUMENTATION PAGE

Form Approved
OMB No. 0704-0188

1. AGENCY USE ONLY (Leave blank)	2. REPORT DATE	3. REPORT TYPE AND DATES COVERED
	30 April 1990	Technical Report 1 Jan.- 31 March 1990

4. TITLE AND SUBTITLE
Composite Ceramic Superconducting Wires for Electric Motor Applications

5. FUNDING NUMBERS
N00014-88-C-0512

6. AUTHOR(S)
J. W. Halloran

7. PERFORMING ORGANIZATION NAME(S) AND ADDRESS(ES)
Ceramics Process Systems Corporation
155 Fortune Boulevard
Milford, MA 01757

8. PERFORMING ORGANIZATION REPORT NUMBER
CPS -90-010

9. SPONSORING/MONITORING AGENCY NAME(S) AND ADDRESS(ES)
Defense Advanced Research Projects Agency
1400 Wilson Boulevard, Arlington, VA 22209

Office of Naval Research
800 North Quincy Street, Arlington, VA 22217-500

10. SPONSORING/MONITORING AGENCY REPORT NUMBER

11. SUPPLEMENTARY NOTES
N/A

12a. DISTRIBUTION/AVAILABILITY STATEMENT
Unlimited

12b. DISTRIBUTION CODE

13. ABSTRACT (Maximum 200 words)

Silver clad polycrystalline Y-123 wire is being fabricated with a continuous reel-to-reel process. Scale-up activities are underway to produce enough wire for the field coils of the HTSC motor. We have produced green HTSC fiber is kilometer lengths, and sintered wires up to 166 meters long. The 77K J_c values are 1000-2800 A/cm^2 in self field. To improve J_c of the Y-123 wire, development began on directional crystallization, including preliminary work at A.D. Little and Oak Ridge National Lab. Large lots of BiSCCO material were produce to fabricated fibers and sintered polycrystalline BiSCCO wire as rolled tape. Work continued in collaboration with Sandia and Los Alamos National Laboratories on rapid thermal processing of Y-123, with most emphasis on characterizing the rapid oxygenation effect.

The design of the HTSC homopolar motor has been improved to increase the output from field coils by using six smaller coils, each with separately optimized current. Motor construction is in progress. Preliminary design is underway on a DC heteropolar motor with HTSC field windings and armature and a brushless "trapped flux permanent magnet" DC motor, in which the field is produced by trapped flux in an HTSC rotor.

14. SUBJECT TERMS
Superconductor, ceramic, motor

15. NUMBER OF PAGES
77

16. PRICE CODE

17. SECURITY CLASSIFICATION OF REPORT	18. SECURITY CLASSIFICATION OF THIS PAGE	19. SECURITY CLASSIFICATION OF ABSTRACT	20. LIMITATION OF ABSTRACT
Unclassified	Unclassified	Unclassified	

COMPOSITE CERAMIC SUPERCONDUCTING WIRES FOR ELECTRIC MOTOR APPLICATIONS

EXECUTIVE SUMMARY

This report describes progress on producing Y-123 wire for an HTSC motor. Wire development emphasized production and scale-up of continuously sintered wire, resulting in the production of a spool of sintered silver clad wire 166 meters long. The wire is being sintered with a continuous process in which spools of green clad fiber are fed into the belt furnace and collected as spools of sintered clad wire at the furnace exit. We have made steady progress toward continuous uninterrupted furnace operation, with the longest run lasting 13 hours before a wire break. We are developing a method to batch annealed long wires in a coiled state. In parallel development of BiSCCO wire, green fiber, green clad wire, and sintered polycrystalline wire has been fabricated from the BiSCCO material. The sintered BiSCCO wire can be cold rolled into a tape.

Development began on post-processing of sintered Y-123 wire by directional crystallization. Melt texturing research work is underway at CPS exploring a range of YBCO compositions and Ag-Pd coatings. Preliminary experiments have been done in preparation for the upcoming subcontracts at A.D. Little and Oak Ridge National Laboratory aimed at melt processing of wires and fibers by floating zone methods and a novel technique of metal jacketed zone melting. Collaborative research continue with Sandia and Los Alamo National Laboratories on rapid thermal processing of Y-123, with most emphasis on characterizing the rapid oxygenation effect.

The design of the HTSC homopolar motor has been improved to increase the output from field coils by using six smaller coils, each with separately optimized current. Motor construction is in progress. Preliminary design is underway on a DC heteropolar motor with HTSC field windings and armature and a brushless "trapped flux permanent magnet" DC motor, in which the field is produced by trapped flux in an HTSC rotor.

TABLE OF CONTENTS

LIST OF FIGURES

LIST OF FIGURES-- continued

COMPOSITE CERAMIC SUPERCONDUCTING WIRES FOR ELECTRIC MOTOR APPLICATIONS

JOHN W. HALLORAN
PRINCIPAL INVESTIGATOR
CERAMICS PROCESS SYSTEMS CORPORATION
MILFORD, MASSACHUSETTS 01757

SECTION 1

GENERAL INTRODUCTION

This Seventh Quarterly Report covers activities during January through March 1990, on a program to develop high temperature superconducting wire by cladding $YBa_2Cu_3O_{7-x}$(Y-123) ceramic fibers with metal, and to use this wire to build a superconducting motor. At this time, the program is being carried out by three subcontractors: CPS Superconductor Corporation (CPSS), a subsidiary of Ceramics Process Systems, is responsible for the development of the wire; Albany International Research Corporation (AIResCo) develops the green fiber spinning and braiding methods, and provides all of the green fibers; and the Emerson Motor Division (EMD) of Emerson Electric, which is building the superconducting motor. Two new subcontracts dealing with improving melt texturing of Y-123 wire are now being negotiated at Arthur D. Little, Inc. and at the HTSC Pilot Center at Oak Ridge National Laboratory. Collaborative research continued on transmission electron microscopy of Y-123 wires at Los Alamos National Laboratory HTSC Pilot Center, and on rapid thermal processing of HTSC wire at Sandia National Laboratory.

The status of the program is compared with individual tasks of the revised Statement of Work in Figures 1.1.1, 1.1.2, and 1.1.3, which show timelines for the major fiber and wire development tasks. The fiber spinning tasks, as shown, involves Y-123 melt spinning and braiding. These tasks will be extended through 1990. The wire tasks are somewhat out of date due to changes as the program has

evolved. The main effort involves silver coated and co-fired monofil wire. The newer activities involving melt texturing, including two planned subcontracts, do not appear in the list of tasks. We are no longer working on multifilament ribbon wire, as it was originally envisioned, as this has been supplanted by work on braids. The HTSC motor tasks are on schedule, except for wire and coil testing, since we have not yet produced coils.

The following sections describe in detail the progress on the wire manufacturing task and the motor design task. Section 2 covers all aspects of the wire manufacturing development, including the fiber spinning work conducted at Albany International Research Corporation in Mansfield, Massachusetts, and the Y-123 powder production, sintering, cladding, and characterization work conducted at CPS Superconductor in Milford, Massachusetts. Section 3 outlines the HTSC motor design activities at Emerson Motor Division in St. Louis, Missouri.

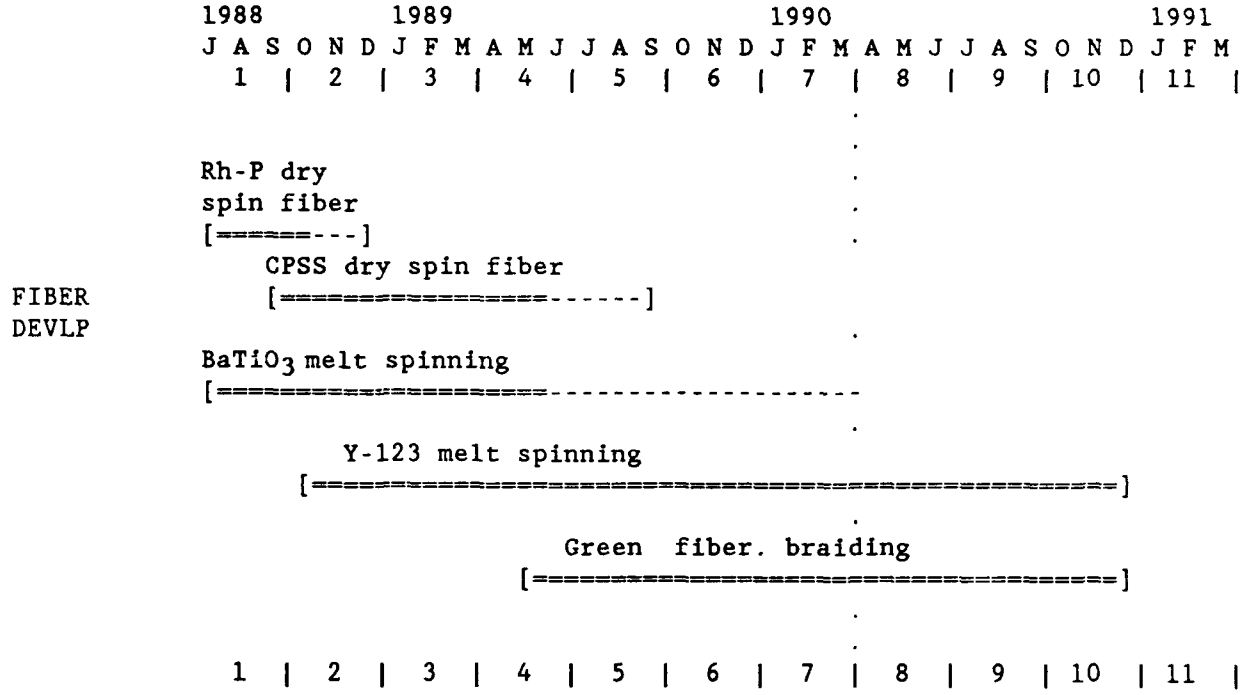

Figure 1.1.1 Revised Project Schedule for Fiber

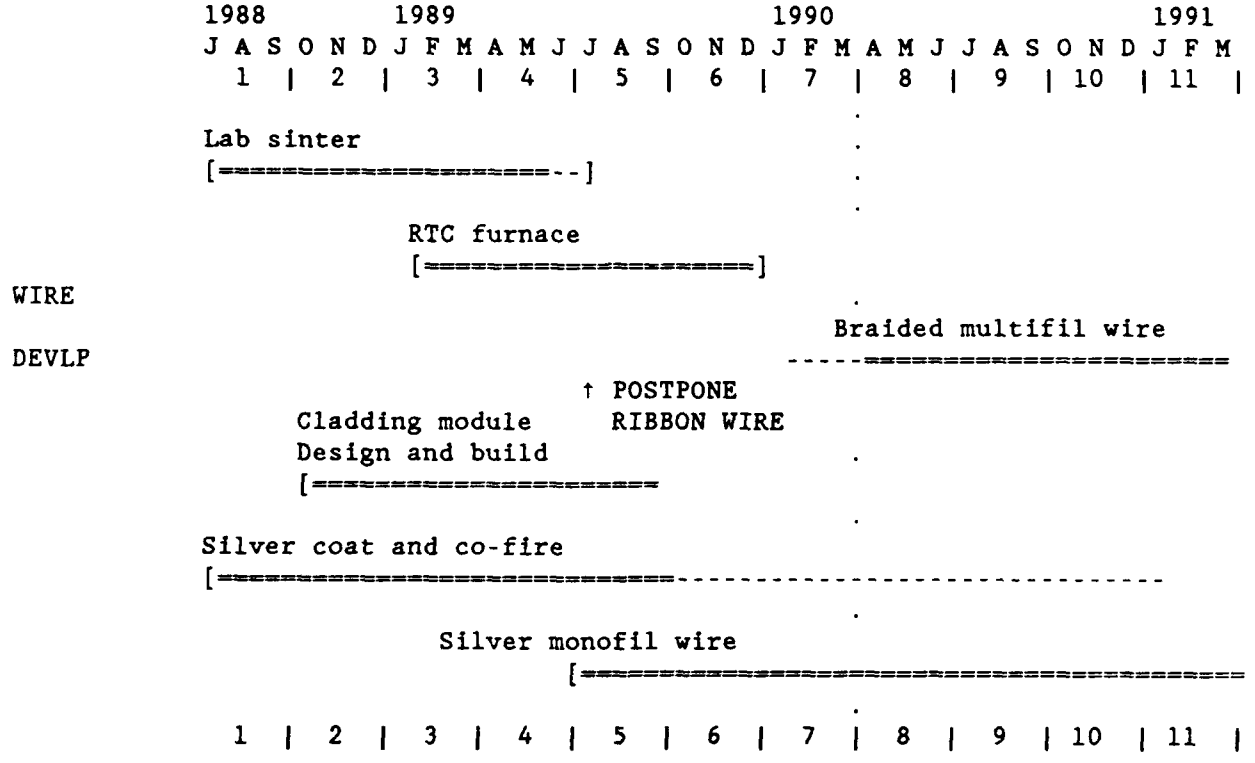

Figure 1.1.2 Revised Project Schedule for Wire Tasks. Note that Ribbon Wire had been postponed in favor of monofil wire

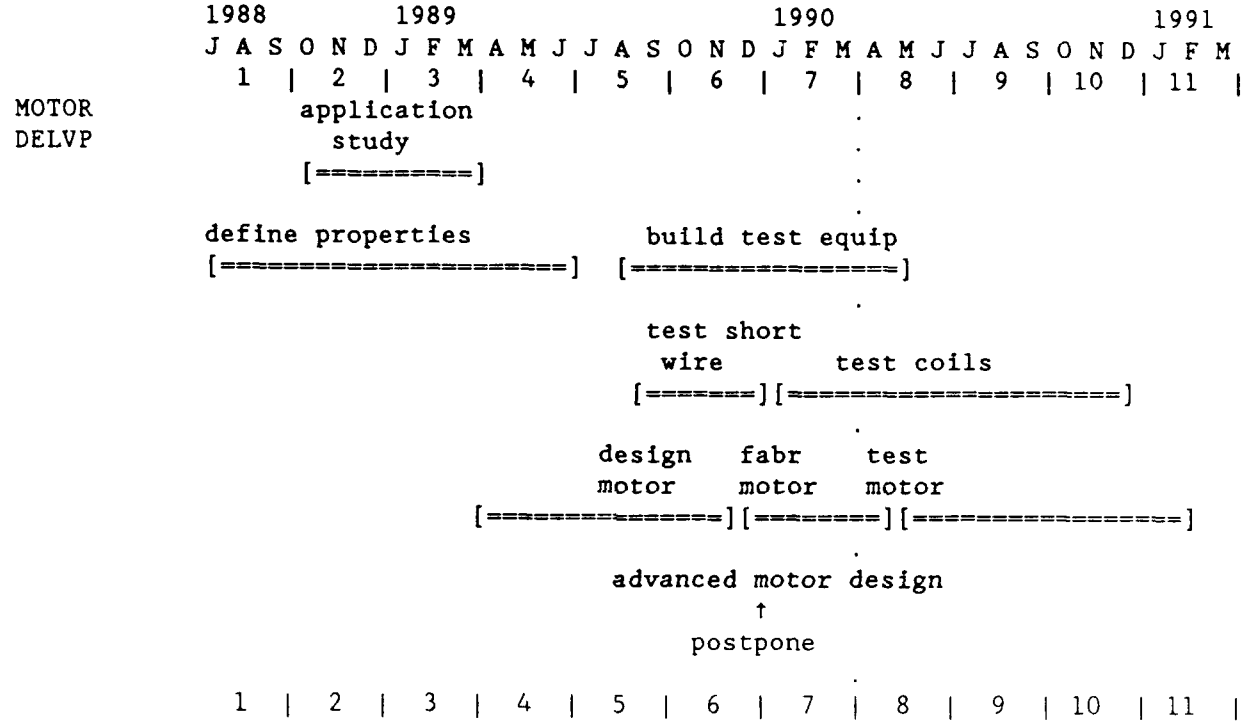

Figure 1.1.3 Project Schedule for HTSC Motor Task

SECTION 2

WIRE FABRICATION

DAVID CHANDLER, JOHN HALLORAN, JAMES HODGE, LORI JO KLEMPTNER,
MATTHEW NEAL, MARK PARISH, HYUN PARK, MICHAEL PARKER, AND VIREN PATHARE
CPS SUPERCONDUCTOR CORPORATION

GEORGE BAKIS, DANA EAGLES, WESLEY ISHIDA, AND STEPHEN TIERNAN
ALBANY INTERNATIONAL RESEARCH CORPORATION

2.1 Introduction and General Comments

This was a quarter with solid progress in our development of HTSC wire from ceramic fiber. Our approach is a three-step process in which we (1) prepare textile-quality "green clad" fiber consisting of melt-spun HTSC green fiber with a particulate silver coating, (2) continuously sinter the fiber to produce silver-clad sintered polycrystalline wire (SP wire), and (3) post-process the polycrystalline wire to make a high critical current density wire. Our primary emphasis has been on Y-123 systems. We have made significant progress on the first two steps and this quarter produced more than 166 meters of sintered polycrystalline Y-123 wire, some of which was wound onto Emerson homopolar motor coil bobbins. We also significantly increased our effort to develop practical post-processing for sintered Y-123 wire to melt texture the Y-123 by directional crystallization. In parallel development to produce sintered wire from the Bi(Pb)SCCO systems, we have determined the powder production and sintering conditions giving fabricated tapes with zero resistance at 108K.

Our principal task is to fabricate the 575 ampere-turn field coils for the Emerson homopolar motor. The design of the coils, based on the $J_c(B)$ performance of our weak-linked SP Y-123 wire, will require six kilometers of the SP wire to

fabricate the two field coils. Each coil is made from six segments wound with 500 meters of wire. Development of scale-up of our SP wire process consumed about 70% of our effort during this quarter.

After completing the extension to our sintering furnace, we resumed continuous sintering of green clad fiber to produce continuous sintered polycrystalline (SP) wire with a reel-to-reel sintering operation. The furnace extension allowed us to accomplish binder burnout and sintering with single pass through extended furnace. This eliminated the need for repeated passes with intermediate spooling, which was our previous semi-continuous sintering method. Since we no longer have to handle the fiber in a fragile partially-sintered condition, most of the fiber breakage problems were avoided.

We now have in place a process in which spools of green clad fiber are fed into the belt furnace and collected as spools of sintered clad wire at the furnace exit. We have made steady progress toward continuous uninterrupted furnace operation. By identifying and solving a series of practical problems, we have been able to run up to 13 hours without a wire-breaking incident.

We now produce hundreds of meters of sintered polycrystalline Y-123 wire (SP wire) which must be oxygen annealed to make it superconducting. At present we still accomplish oxygen anneals but cutting the wire into short pieces to be annealed in a tube furnace. We are developing annealing procedures for continuous wire batch annealed as coils of sintered wire. We have designed and built a high temperature alloy retort to allow us to anneal large spools of wire, and expect to have this process operational during the next quarter.

The balance of our effort this quarter was about evenly split between melt texturing of Y-123 and developing SP wire in the Bi(Pb)SCCO system. The melt texturing work involved static furnace anneals of pellets and fibers at CPS

exploring a range of YBCO compositions and Ag-Pd coatings. Preliminary experiments were done in preparation for the upcoming subcontracts at A.D. Little and Oak Ridge National Laboratory aimed at melt processing of wires and fibers. Also, work continued in collaboration with Sandia and Los Alamos National Laboratories on rapid thermal processing of Y-123, with most emphasis on characterizing the rapid oxygenation effect.

The detailed progress reports for each of the four wire process steps are presented in Sections 2.2 through 2.5.

2.2 Fiber Preparation

2.2.1 Introduction

Activities related to powder preparation and fiber processing are reported in this section. Production of materials in the Y-123 system included standard 1.6 micron stoichiometric powder and a variety of experimental off-stoichiometric compositions, largely for melt texturing work. Development of processes for BiSCCO materials received more attention this quarter, leading to spin runs of improved compositions. The fiber spinning process was further developed, with emphasis on green fibers with 60 volume percent Y-123 loadings, exploration of alternative polymers, and the first efforts at multifilamentary spinning.

2.2.2 Powder production

Production of Y-123 powder continued routinely to supply project needs. We continue to examine process variables and techniques to improve the manufacturing process and powder quality, as well as examine environmental effects. Some rather more fundamental research has been underway to characterize the gas-solid and solid-solid reactions during calcination of Y-123. This has included collaborative research with high temperature X-ray diffraction with Cam

Hubbard at the High Temperature Materials Laboratory at Oak Ridge National Laboratory. This work will be reported in separate publications.

Several processes were examined for producing Y-124. We also prepared approximately one kilogram quantities of Y-211 and barium cuprate to supply off-stoichiometric materials for melt processing.

We significantly increased effort directed at bismuth cuprate systems, with emphasis on the lead doped Bi(Pb)SCCO-2223 system, producing a number of compositions around $Bi_{2-x}Pb_xCa_{2+y}Sr_{2.0}Cu_{3+z}O_\delta$. This involved initial work with melt spun BiSCCO green fiber, which we used to produce silver clad sintered wire, and more detailed work to develop compositions and heat treatments.

The powder lot used for the melt spun fiber was prepared by milling a mixture of oxides and carbonates with composition Bi/Pb/Sr/Ca/Cu of 3.8/0.8/4/5/7. A 0.8 kg lot was calcined at 825°C for 15 hours in flowing air. The calcined product was a two phase mixture of Bi-2122 and a calcium strontium plumbate. This powder was used to melt spin several large spools of 125-micron fiber and smaller quantity of 1375-micron fiber.

Since melt spinning of green fibers is inconvenient and costly for screening many small samples of variable composition, the composition development was conducted with tape cast sheets. Compositions were formulated varying the lead substitution and copper content as listed in Table 2.1. Powder was calcined at 775°C in air for six hours, wet milled in solvent, and tape cast. Tape samples were supported on silver foil during sintering. Figure 2.1.1 shows the AC susceptibility of the sintered tapes as a function of composition. At these calcining and sintering conditions, the best composition is BP-2, or a $Bi_{1.7}Pb_{0.3}$-2223.

TABLE 2.1

BiSCCO COMPOSITIONS

$Bi_{2-x}Pb_xCa_{2+y}Sr_{2.0}Cu_{3+z}O_\delta$

notation	x	y	z
BP-1	0.2	0	0
BP-2	0.3	0	0
BP-3	0.4	0	0
BP-4	0.6	0	0
BP-5	0.8	0	0
BP-6	0.3	0.2	0
BP-7	0.3	0.4	0
BP-8	0.3	0	1

Subseqent work focused on the BP-2 composition. A series of experiments were conducted to define effective calcining temperature and times. Figure 2.1.2 shows AC susceptibility as a function of calcination temperature for tapes sintered at 865°C for 12 hours, showing better properties with calcination in the 750-775°C range. A tape with the BP-2 composition, calcined and sintered under these conditions had an onset at 110K and zero resistance at 98K, as shown in Figure 2.2.3. Repeated sintering improved the properties. Figure 2.1.4 shows the AC susceptibility for a variety of samples, indicating a significant improvement in twice-sintered tapes.

Based on this information, three 0.75 kilogram lots of BiSCCO powder were prepared for green fiber spinning. The results are reported later in this section and in Section 2.3.5.

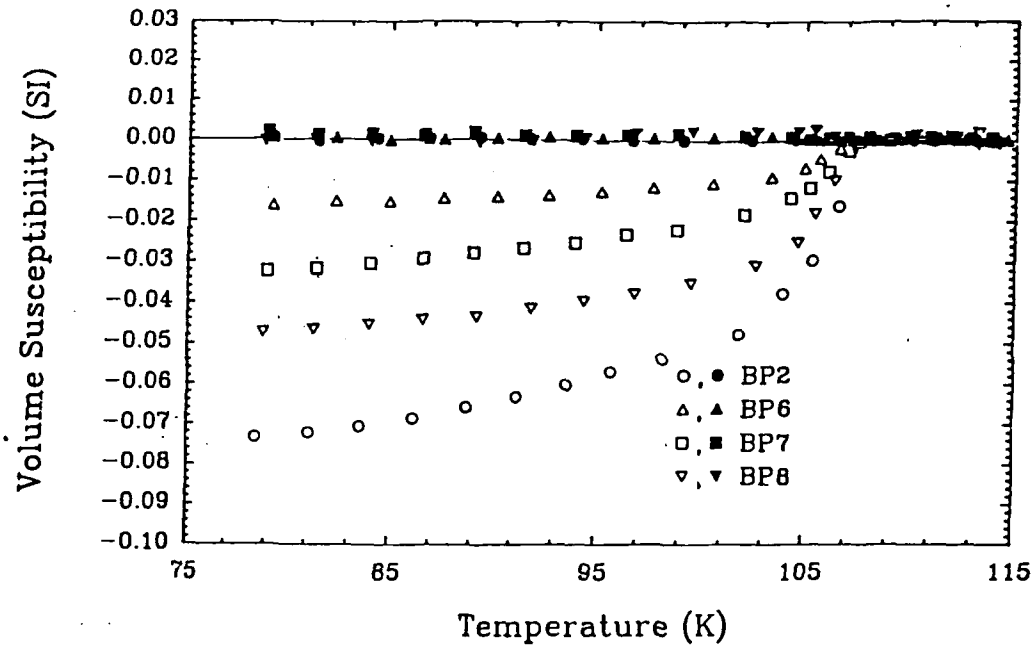

Figure 2.1.1 Real and Imaginary AC Susceptibility for Bi(Pb)SCCO Tapes Calcined at 775°C for 6 Hours and Sintered at 865°C for 12 Hours as a Function of Composition. Compositions are Defined in Table 2.1

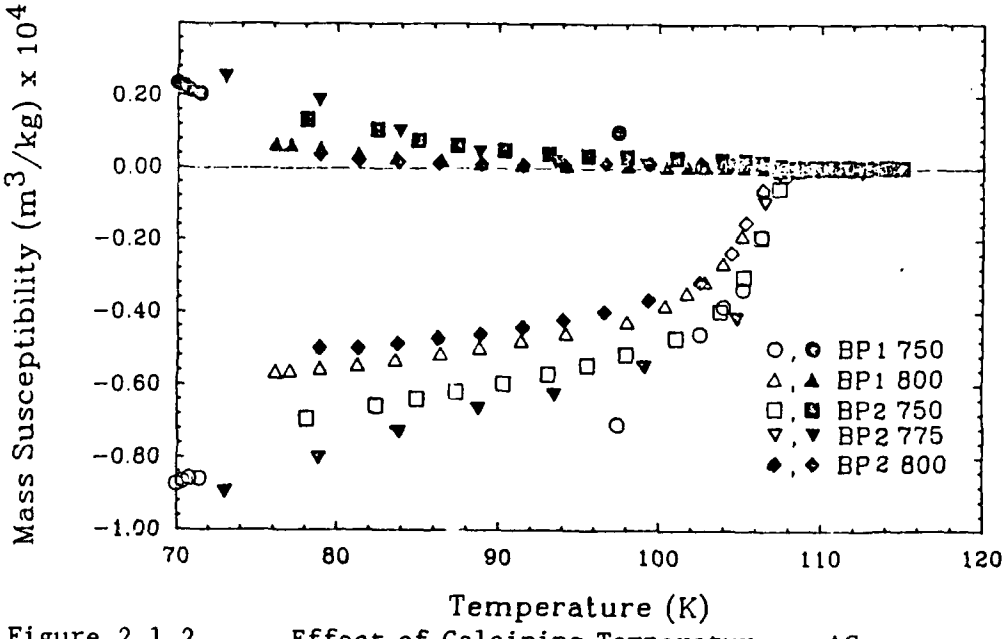

Figure 2.1.2 Effect of Calcining Temperature on AC Susceptibility for Bi(Pb)SCCO Tapes Sintered at 865°C

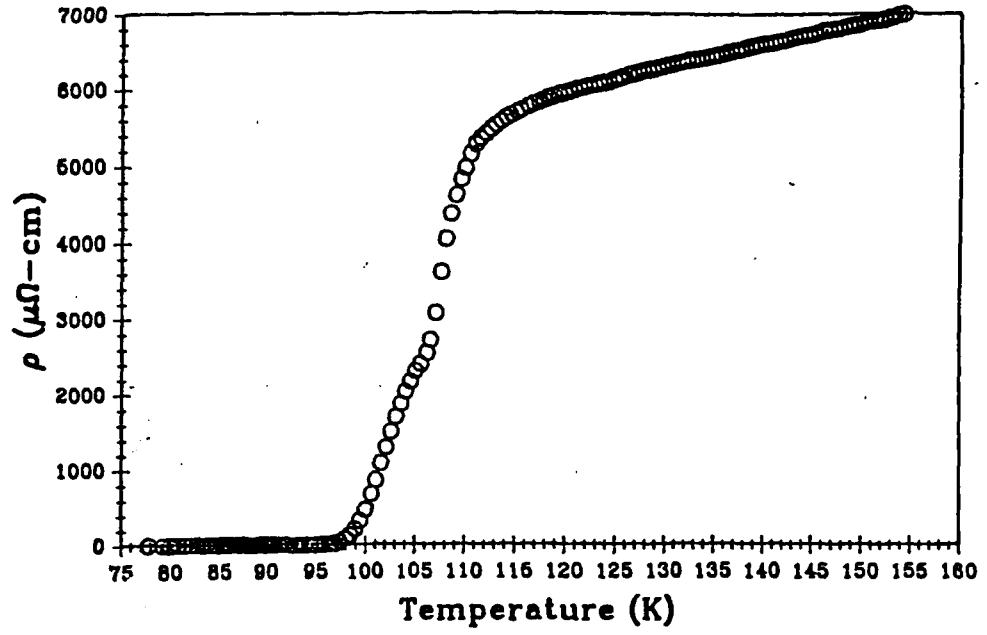

Figure 2.1.3 Resistive Transition for Bi(Pb)SCCO Tape Calcined at 775°C and Sintered at 865°C. Composition $Bi_{1.7}Pb_{0.3}Ca_2Sr_2Cu_3O_\delta$

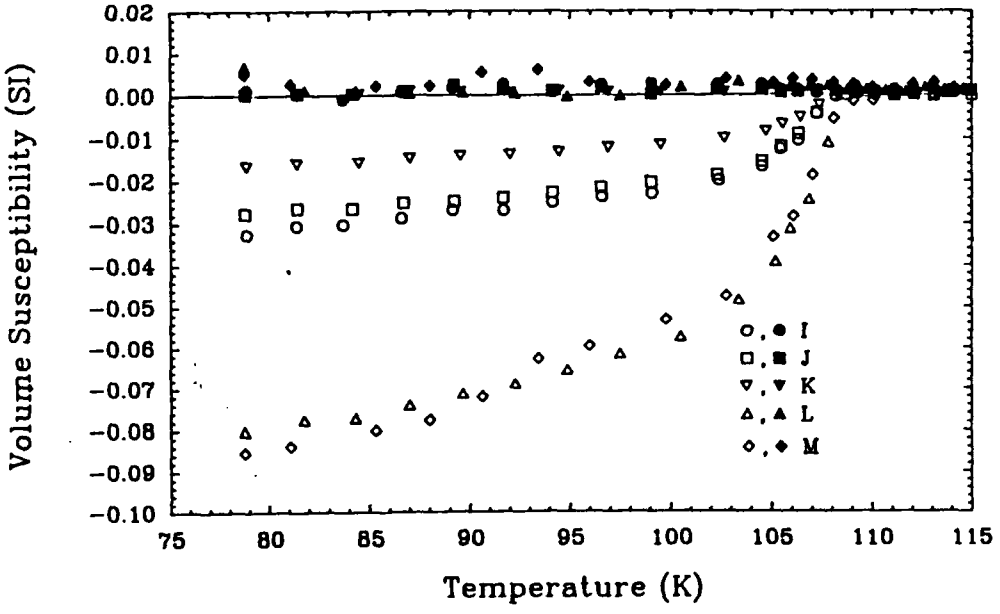

Figure 2.1.4 Effect of Repeated Sintering on Susceptibility of BiSCCO Tapes. All Samples sintered 12 hours at 865°C, but Samples L and M Were Sintered Twice. Calcination Temperatures: 775°C for I,L, 800°C for J,M and 825°C for K. Composition $Bi_{1.7}Pb_{0.3}Ca_2Sr_2Cu_3O_\delta$

2.2.3 Green fiber spinning

Most efforts in green fiber spinning concentrated on producing Y-123 green fiber. The "standard" green fiber continued to be a 125-micron diameter monofilament prepared from the 1.6 micron stoichiometric powder using the high density polyethylene (HDPE) polymer system at a solids loading of 50 volume percent. Each one of these characteristics was varied in a series of experiments investigating particle size, polymer system, and solids loading.

2.2.3.1 Experimental fibers

Green fiber spinning experiments were done with powder air-classified to a finer grade, a coarser grade, and a bimodal mixture. These experimental powders compounded and spun well, to form 125-micron diameter green fibers with lengths in excess of 1.3 kilometers.

Preliminary data on the properties of sintered bare fibers, reported last Quarter, showed significantly higher critical current density from fibers at 60v% solids loading. We attempted to evaluate whether we could adopt 60 volume percent as our standard loading. Several spinning experiments were undertaken at 60v% to further develop the higher solids green fiber. It proved to be difficult to reproduce 60v% Y-123 green fibers with the standard HDPE formulation. Spinning rates were much slower, and significant differences in spinnability were seen between powder lots. Some powder lots had satisfactory behavior during compounding and spinning, but two lots were particularly difficult to spin. Preliminary data suggest that the powder lots with poor spinnability had specific surface area in the high end of our specification range ($2.3+/-0.2 m^2/gm$), while the satisfactory lots tended to the lower end of

the surface area range. We are continuing this activity.

Yanagisawa and his colleagues at Ashahi Glass[1] reported improved melting behavior in compositions containing 211 phase. Fibers with composition 123+30 wt% 211 were prepared for melt texturing and RTP experiments. The feed stock was prepared by mixing standard grade 123 powder with calcined phase pure 211, followed by jet milling of the mixture to reduce the particle size of the 211 phase. This mixture behaved similarly to the usual 123 powder during compounding and spinning. Spools were collected at 125-micron and 375-micron diameters.

Composite green fibers were fabricated from 123+30 v%Ag, using a mixture of standard 123 powder and 2-micron spherical silver powder. Compounding and spinning of this mixture was similar to simple 123, but fiber breakage during takeup limited the length of continuous filament to a few hundred meters.

Three spinning runs were conducted with BiSCCO powders to produce 125-micron fiber and 1375-micron rod. These BiSCCO materials seem to be very easy to spin using the conventional HDPE formulation. Excellent fiber was produced from both hand ground powder and jet milled powder, indicating that spinnability is not sensitive to particle size. The third powder lot was used to prepare a very large quantity of fiber consisting of several 1.5 kilometer spools totaling more than 5 kilometers of green fiber.

2.2.3.2 Alternate polymer systems

High density polyethylene (HDPE) is a reasonably satisfactory carrier

---

[1]. E. Yanagisawa et al., Asahi Glass Company Research Center, "Synthesis of Unidirectionally Solidified YBCO Bulk Superconductors with High Critical Current Density", paper M4.3 at the Materials Research Society Meeting, Boston, MA, November 28, 1989

polymer for green fiber, exhibit good compounding and spinnability, good green strength, and acceptable binder burnout characteristics. However, it is not ideal, since it offers limited draw, which frustrates attempts to routinely spin fibers finer than 100 microns. It is a crystalline polymer, so drawn fibers have excessive shrinkage due to relaxation during the initial stages of heating. Finally, we find that slow heating is required for successful burnout, which will eventually limit wire production rate. Consequently we continue to evaluate alternatives, emphasizing amorphous polymers from systems we expect might have more facile burnout.

Polyvinyl butyral (PVB) has proved a very effective carrier polymer for barium titanate, a surrogate we have used in place of costly Y-123 for spinning experiments. Unfortunately, Y-123 fibers prepared with PVB have so far demonstrated inferior electrical properties. Some observations indicated that the critical current density of PVB-based fibers depended upon the type of lubricant used during spinning. Fibers were spun with several lubricants and different grades of PVB to yield quite good green fibers. The electrical properties of the wires after sintering are still under evaluation. One PVB-based system has produced green fibers with 60 volume percent barium titanate with exceptional green strength. When this formulation was attempted with 60 volume percent Y-123, however, we were unable to produce a homogeneous blend during compounding. This was surprising, since we have usually been able to reproduce barium titanate results with Y-123 at our typical solids loading of 50 volume percent. It appears that 60 v% solids is near the maximum solids loading for our present melt spinning process, which exaggerates differences between powders which would not be noticed at lower solids content.

Acrylics and methacrylates may be promising, as certain acrylic binders

are known to have clean burnout in ceramics. We successfully spun flexible green fiber from an acrylic system, but the fiber had poor green strength. Further attempts were made to produce flexible fiber with methacrylates, using several new grades of polymer and lubricant but, as before, all of the methacrylate fibers have been too brittle.

2.2.3.3 Multifilament Fiber Development

Finer green fibers will make more flexible wire. Currently, monofilament green fiber cannot be practically handled at diameters finer than 125-microns, primarily because the tensile loads associated with spooling and handling break the finer fibers. The solution is to prepare multifilamentary tows of finer fibers, which distribute the handling loads onto a large number of filaments.

We have had preliminary success on multifilament spinning using a die with six 125-micron holes. The effort was aimed at producing the fine filament diameters, so a 50 volume% barium titanate/PVB formulation with good drawdown ability was chosen. Multifilament fiber was collected continuously with diameters as small as 75 microns per filament.

2.3 Sintering and Cladding

We increased the scale of all of our processes this quarter, producing more than a kilometer of green clad fiber, with various types of cladding, which was used in a large number of sintering experiments, as well as the production of 166 meters of sintered Y-123 SP wire. Figure 2.3.1 is a photograph of some of this wire wound 20 turns around a 30 cm diameter spool. A typical cross section of recent wire is shown in Figure 2.3.2.

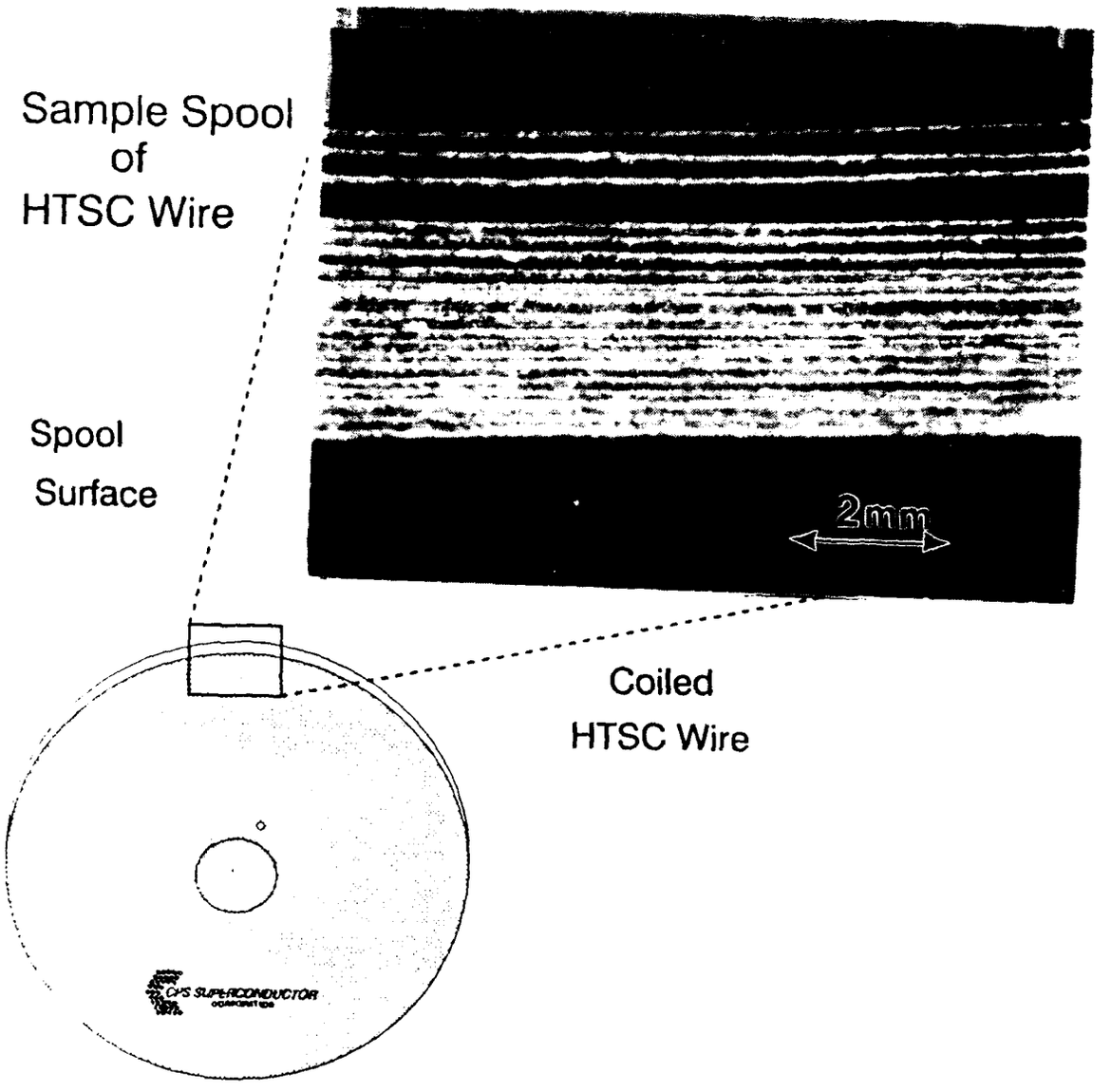

Figure 2.3.1 Photograph Showing part of the Windings of Sintered Silver Clad Polycrystalline Y-123 Wire Wound on a 30-cm Diameter Spool (12x)

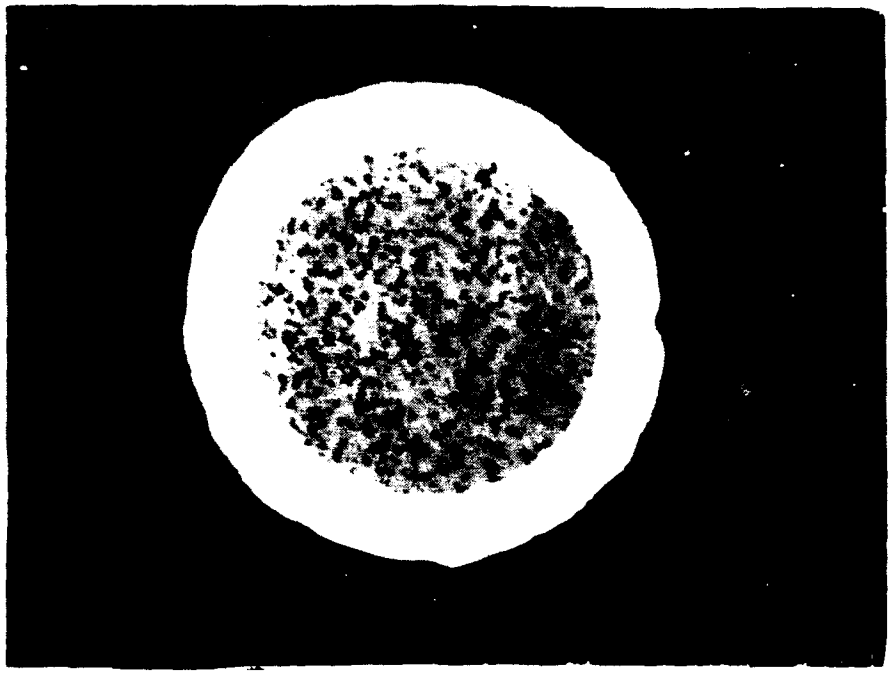

Figure 2.3.2 Cross Section of Recent Ag-Clad Sintered Polycrystalline Y-123 Wire

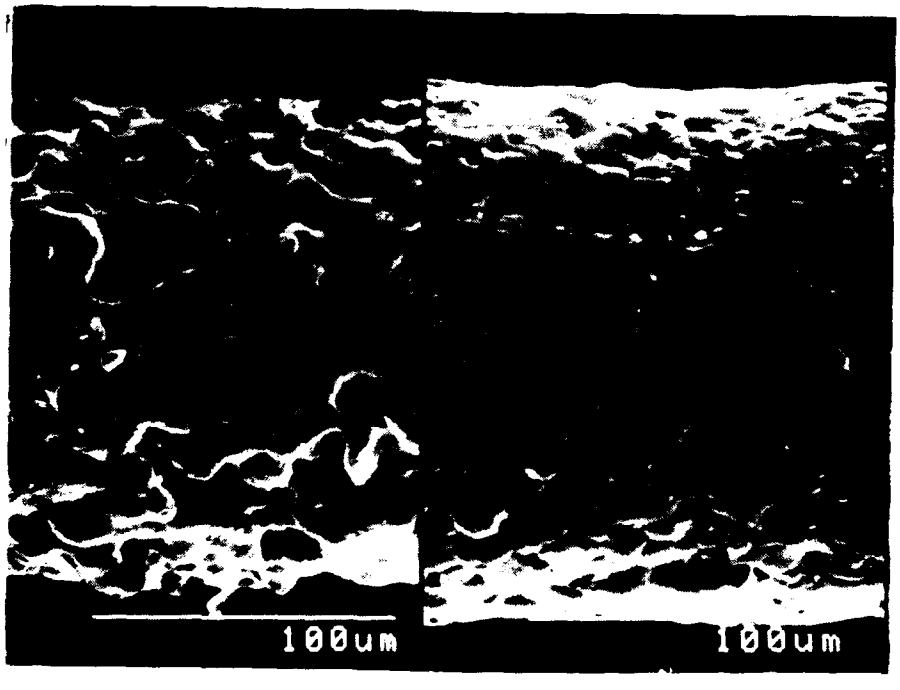

Figure 2.3.3 Comparison of the Porous Silver Coatings form Spherical Powders (left) with Dense Silver Coatings from Flakey Silver Powders (right)

2.3.1 Cladding and co-firing

The most important event in the green cladding and co-firing was improved understanding of the influence of the coating on binder burnout and sintering, and realization that flakey and spherical powders give distinctly different coatings. These are illustrated in Figure 2.3., comparing sintered silver coating prepared with flakey and spherical powders. Spherical powders give porous coatings, even when thick. During initial heating BBO is noticeably easier with the spherical Ag powder green coating, as the green coating is more permeable. The sintered coating is porous, which has the advantage of easier oxygen intercalation. We see higher J_c values in these wires after our usual 10 hr oxygen anneal. However, the porous coatings not as strong, so the wire is more fragile. Since they are obviously not hermetic, they probably offer little protection from environmental degradation. The flakey particles give a dense silver cladding which is much stronger and hermetic against environmental degradation. The disadvantage is the cladding is a greater barrier to oxygen diffusion during the intercalation anneal. Indeed, while relatively thin 7-micron coatings have given acceptable J_c values, wires with thicker coatings have not yet been successfully annealed. Binder burnout is also more difficult with the flakey silver coatings.

2.3.1.1 Green Cladding

The process for green cladding is essentially the same a previously reported. The process and the cladding machine have been upgraded and the scale at which we operate has been increased. More than 1.2 kilometers of green clad fiber were produced to support wire sintering work and supply green clad

material for braiding. To improve the cladding apparatus, we have designed a synchronized pay-out and take-up spooling system which, when combined with neatly would green fiber packages, will permit the green cladding operation to be conducted without the need for constant operator attention.

2.3.2 Continuous sintering

The larger scale continuous sintering facility was brought up during this quarter, featuring a large extension of the binder burnout section built onto the RTC furnace. We have previously reported on the design and building of the furnace extension. During this quarter the assembly was completed and it was brought into service. The furnace extension is 3.3 meters long with five separately controllable zones with resistance heating and atmosphere control which can be independent of the RTC furnace, which now serves as the high heat section. The complete facility is about 5.5 meters long with eight heating zones. Green fibers are payed out onto a woven Nextel belt to be carried through the burnout section, sintering section, and cooling zone, and taken up on a spool at the exit. A new rubber roll drive mechanism has greatly reduced the wear of the Nextel belt.

An important part of the sintering facility is the speed control system which synchronizes the speeds of the payout spool, take up spool, Nextel drive, and the RTC metal mesh belt drive. After these systems were installed and adjusted it was possible to run the machine unattended for long periods. In practice, the take-up spooling rate is matched to the belt speed to take up the sintered wire without slack. The pay-out spooling rate is adjusted to maintain a constant slack. The speeds of the pay-out and take-up are not the same. Usually, the pay-out speed is faster by a factor of 1.045, suggesting that the

fiber undergoes 4.5% axial shrinkage during continuous sintering.

The new sintering facility worked properly on its first trial. The first continuous sintering run involved simple bare Y-123 green fiber to establish a baseline. We were pleased to find the sintered bare fiber seemed to be much stronger than it was old the previous semicontinuous sintering treatments. We could handle the 100-micron sintered quite easily and hold 2-meter lengths by the ends. In contrast, the bare fibers sintered according to the same schedule by the old semicontinuous method were much more fragile. In fact, the bare fiber could be easily spooled, so new take-up spooling procedures could be developed using simple bare fiber. Apparently true continuous burnout and sintering is much more gentle than our previous semicontinuous sintering method, which involved one or more intermediate spoolings of partially sintered fiber.

Once the facility was operating, the main thrust of our activity was scaling up production of an interim "standard" wire. We actually have no such standard, since the green fiber, green cladding, and process is continually being improved, and the new facility created opportunities for further improvements. After a series of small scale experiments, the interim standard was chosen for production of at least 150 meters of sintered wire. The 150 meter wire was made from a particular lot of 60 vol% green fiber, green clad with silver using flaky particle morphology (sintered clad thickness 20 micron), sintered with a conservative binder burnout profile and peak sintering temperature of 920°C at a belt speed corresponding to about 30 minutes in the sintering zone.

Production of kilometer-long continuous wire will require the sintering facility to operate 24 hours per day unattended by operators. We have made significant progress in unattended operation. One of the early attempts at

unattended operation lasted two hours before a problem interrupted the run, but by the end of March we were able to run 12.6 hours without an interruption. Progress has come by solving a series of problems. These have been very practical matters involving such things as guiding the green fiber from the spool to the belt, arranging for the green fiber to pay off from the spool without tangles, etc. For example, many of our current difficulties are related to the neatness of the green fiber on the spools. Typical textile fibers are wound with high tension to give a tight and orderly "package" on the spool. Green fibers must be wound with very low tension, so the package is loose and prone to tangles. Our green cladding and re-spooling operations are now done by hand and wound in a random fashion. We now find this unacceptable for unattended operation, and are building special low tension spoolers to produce the orderly packages we need.

With the present conservative sintering profile, belt speed is slow, so production rate is increased by using several parallel fiber lines. We routinely do two lines, although four have been successfully done. The 166 meters of sintered wire was produced by splicing a number of smaller lengths. The longest continuous wire to date is 21 meters.

2.3.3 Processing Experiments on Co-Fired Y-123 Wire

We have conducted extensive sintering trials to evaluate substrate green fiber, examine the type and thickness of silver cladding, and develop appropriate burnout and sintering schedules. The main theme of the green fiber work is comparing the properties of wires made from the 50- and 60 volume percent green fibers. Our intention is to decide whether to adopt 60 percent solids loading as the standard. At present, the data is incomplete and we are

unable to make convincing comparisons.

The thickness and type of silver cladding is critical to the processing, as the burnout, sintering, and annealing steps are all strongly influenced by the cladding variables. The type of cladding must be standardized before these steps can be optimized. The optimal cladding thickness is a compromise between strength and handling characteristics, which are better with thicker coatings, and sintering (burnout) belt speed and annealing rate, which must be slower with thicker claddings. We have not yet settled on a cladding type. Much of our effort had been directed to spherical silver powders which gave the porous cladding, as these wires showed the best electrical properties. Later we decided to emphasize flakey silver claddings, which were dense and strong. The optimal cladding thickness has not yet been determined. For the present we have adopted an cladding thickness around 20 microns, chosen on the basis of the observation that wires with claddings at least this thick are stronger and exhibit apparent ductility rather than brittle fracture.[2]

All of our sintered wires are now annealed in a batch mode using a relatively small tube furnace. This requires cutting the wire into 3-10 cm lengths. Obviously, this is only appropriate for experimental purposes, but it has sufficed when we were exploring many process variables. The batch anneals are based on methods developed for bare Y-123 fibers, and typically involve heating in flowing oxygen near 500°C overnight. For our most common "standard anneal" the tube furnace is loaded cold, flushed with oxygen and ramped quickly to 820°C, cooled at 150°C/hr to 520°C, where it is held for 10 hours, followed

---

[2]. These wires appear to be ductile, and can be bent plasticly without gross failure. Of course the brittle ceramic substrate fractures during bending, but the cladding holds the composite wire together. Wires with thinner claddings break in a brittle fashion and are noticeably weaker.

by cooling at 50°C/hr to 300°C.

To develop an annealing cycle for the interim standard wire, we have initiated a thorough annealing study to compare the electrical properties of several varieties of wire as a function of clad thickness, dense vs. porous silver cladding, and temperature-time profile. The results will not be available until next quarter. This information will be used to determine the temperature-time schedule for large scale annealing of wire.

Large scale annealing will be accomplished by annealing spools of sintered wire in a batch mode. Several large metal spools have been made from inconel, modeled on the large diameter plastic spools we presently used for take-up of sintered wire. The plan is to transfer a kilometer or more of sintered wire onto the inconel spools and anneal the wire in oxygen in a periodic furnace. We began experiments to qualify a rather large Bailey kiln as an annealing furnace. For safe operation in oxygen, we have designed and built an inconel retort to fit inside the 80 cm diameter by 100 cm deep cylindrical hearth of the Bailey. The retort will hold three of the inconel spools. This system will be operational next quarter.

2.3.4 Continuous Sintering of Y-123 Braids

Experiments continued on multifilamentary wire produced from braided green clad fiber. Figure 2.3.4 is a photograph of a recent sintered braid made with green clad fiber. A seventeen-filament braid, produced from green clad 125-micron fiber, has been successfully sintered in the continuous furnace at lengths on the order of one meter. The sintered microstructure looks good, and properties are being evaluated. At the 125-micron diameter, sintered braids are too inflexible to collect on a spool. We are now proceeding with longer braids.

2.3.5 Processing of BiSCCO Fiber and Wire

During the last quarter we have began to apply our fiber process to the BiSCCO system. Using an early composition and calcining process, we produced about a kilogram of $Bi_{0.7}Pb_{0.3}$-2223powder to enable the spinning of a spool of 125-micron BiSCCO green fiber. With this fiber we were able to demonstrate each of the process steps for sintered wire. About 30 meters of BiSCCO fiber were green clad with 25 microns of spherical silver. A 10 meter sample of green clad fiber was continuously sintered at a peak temperature of 840°C, which resulted in a coherent silver clad wire. The wire was used as feedstock for experiments on anneals aimed at developing the 110K 2223 phase, but we were unable to achieve zero resistance from this early grade of wire. Subsequent experiments with small lots have resulted in zero resistance tapes above 100K, as reported in Section 2.2.2. Early experiments with the SP BiSCCO wire demonstrated that the silver clad wire could be cold rolled to make a tape shaped wire. This was very encouraging, and forms the prototype of our future activities with this material. Figure 2.3.5 shows the BiSCCO wire in each stage of the process. We expect to produce rolled tape BiSCCO wire from monofilament wire and as multifilamentary tape by rolling braided wire.

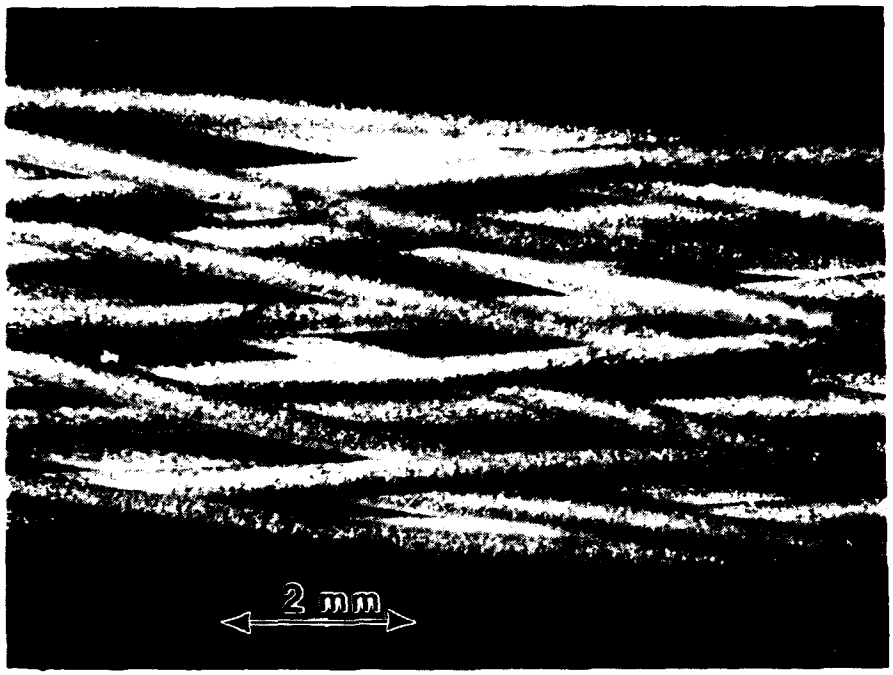

Figure 2.3.4 Seventeen Filament Braid of Silver Clad Polycrystalline Y-123 Wire Continuously Sintered using Braided Green Clad Fiber

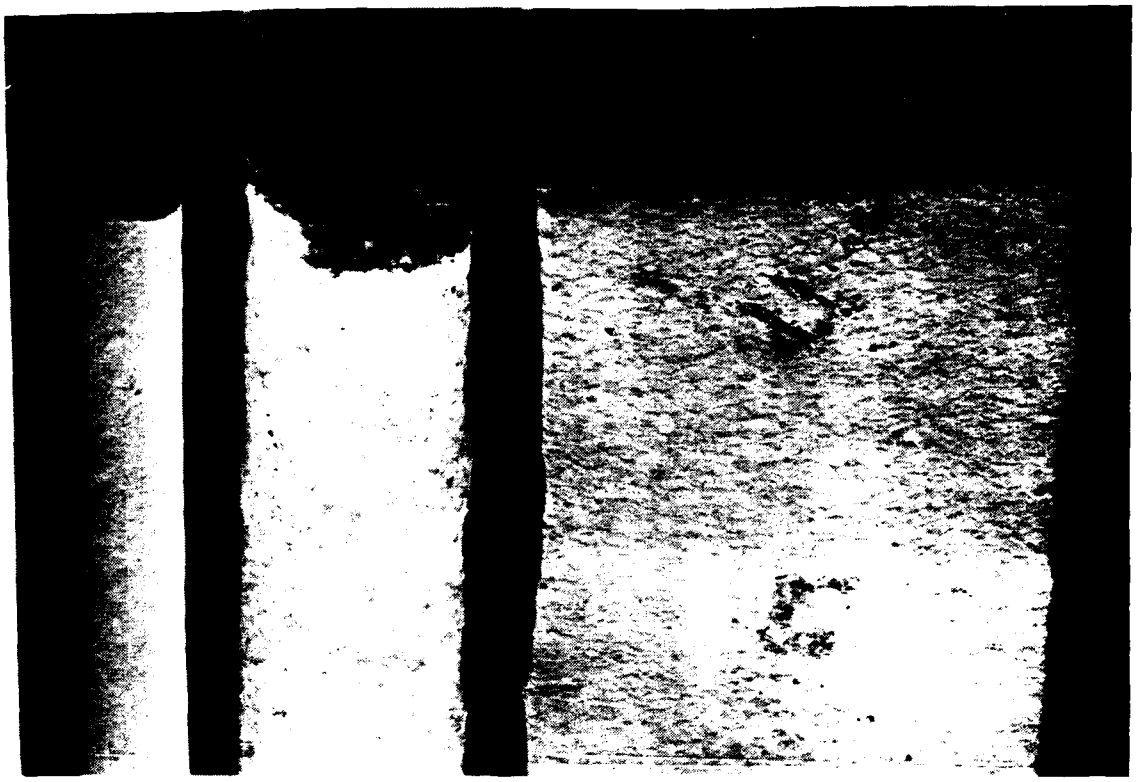

Figure 2.3.5 Stages in the Production of Prototype BiSCCO Wire. From Left: Green fiber, Green Clad Fiber, Sintered Wire after Rolling

2.4 Electrical Characterization

The majority of the effort in electrical characterization was the determination of self field transport critical current densities in support of the wire development effort, involving about 300 measurements. Magnetic susceptibility measurements were used more commonly, and were correlated with transport data.

The self field 77K J_c values remain about the same, with typical "good" wires in the range of 1500-2000 A/cm^2. As we made a major change in our wire-- moving from porous silver to dense silver cladding -- most of our wires had much lower critical current density. We expect the new wires to return to the 2000 A/cm^2 range after we adjust the oxygen annealing procedure for the dense silver.

Much of the measurement lab time was devoted to characterizing experimental wire and evaluating BiSCCO tape. Two large formal experiments were undertaken. The first, an annealing study, is still in progress. The second was a study of spacial and statistical variations, reported in Section 2.4.2.

2.4.1 Measurement Technique

Measurement techniques for transport are essentially the same as previously reported. Most work is now on silver clad wires, so contact is straightforward. Note that we define our current densities on the basis of the Y-123 cross sectional area, rather than the whole wire, to facilitate comparisons with different cladding thicknesses. Magnetic susceptibility data on our sintered filaments were taken with the Lake Shore Cryotronics Model 7000-1 AC Susceptometer, which was received during this quarter. This instrument has

already become a workhorse in our laboratory. The specimen is typically several filaments mounted coaxial with the magnetic field, although we are able to measure a single filament. Volume susceptibility at 200 Hz is calculated on a sample volume on the order of a few tenths of cubic millimeters (corresponding to a sample mass around a milligram). Typically the measurements are done a 1G or 0.1G.

2.4.2 Statistical and Spacial Variations in Critical Current Density

In previous quarterly reports we presented data on specimen-to-specimen variations and within-specimen variations in J_c for bare Y-123 filaments. We have extended this to include Ag-clad wires. The intent was to examine a rather large sample of "identical" wires and look at gage length effects in longer wires. The study was done on a large lot of wires with a 10-micron thick porous silver cladding made with the spherical silver powder. Unfortunately, this particular wire lot was rather low quality, so most of the transport J_c values were around 500 A/cm^2.

Green clad fiber was sintered continuously according to the standard profile, with the peak sintering temperature zones corresponding to 30 minutes at 920°C. The 3-meter long sintered wire was cut into a large number of "small" pieces (for 2-cm. gage length tests) and "long" pieces (for multiple contact experiments up to an 8-cm gage length). All of the wires were annealed together in a tube furnace for the then-standard oxygen anneal: heat to 830°C; ramp down to 520°C at 50°C/hr; dwell 10 hours at 520°; furnace cool. The short wires were mounted for conventional 4-point measurements, and the long wires were mounted with six contacts, allowing 4-point measurements to be taken over 2-,4-, and 8-cm gage lengths.

The specimen-to-specimen scatter in J_c values fit a normal distribution.

Figure 2.4.1 shows the distribution function for the 2-cm gage lengths data from the short wires. The mean is 730 A/cm^2 with a standard deviation of 77 A/cm^2. This can be compared with the long wire data over the 2-cm gage length. One expects these to be identical, but Figure 2.4.2 shows a significantly lower mean of 550 A/cm^2 and a larger standard deviation of 182 A/cm^2. It is surprising that 2-cm segments of long wires could be different from 2-cm segments of short wires.

The long wire data shows that longer segments tend to have lower mean J_c values and less scatter, as might be expected. This appears in Figure 2.4.3, comparing the 2-cm, 4-cm, and 8-cm gage lengths based on the multiple contacts experiments on three long wires.

The multiple contact wires provided an opportunity for exploring spacial variations three of these wires. Figure 2.4.4 illustrates the values obtained when J_c was measured over five of the combinations for 4-point measurements.[3] This shows variations of more than a factor of two from one location to another. For example, in wire #3, the first 2-cm segment (2-3) had a J_c of only 255 A/cm^2, while the next 2-cm segment (303) carried 624 A/cm^2. We are investigating the origin of this variation.

The longer gage length critical current density is not quite the same as the lowest local J_c value. Although the criterion for J_c is an electric field of 1 microvolt/cm, one actually measures the potential difference between two leads, and uses the gage length to obtain an average field $E_{av}=\delta V/L$. To illustrate the difference we have in Figure 2.4.5 the actual voltage differences measured at the 4 taps on one of the long wires. The upper right

---

[3]. Each wire had six leads. Leads 1 and 6 were used for current leads, while we measured the voltage across lead pairs 2-3, 2-4, 2-5, 3-4, and 4-5. Each J_c corresponds to the usual 1 microvolt/cm criterion.

plot shows the distribution at a current density of 305 A/cm^2 (well below the critical current density for the wire). Notice that three sections have zero resistance, while the left segment, at an average field of 1.5μV/cm, is beyond the criterion. At a higher current density of 407 A/cm^2 (upper right) the whole wire is near its J_c. The middle segment, however, is still at zero resistance. This persists at 509 A/cm, with the center still superconducting while the wire is well beyond J_c. Finally, notice that the voltage distribution is still nonuniform at 1005 A/cm^2, even though the current density is far beyond the J_c of all segments.

The origin of the spacial variation and specimen-to-specimen variations are still obscure. We have, however, that the self field transport J_c correlates well to the real AC volume susceptibility at 77K. Figure 2.4.6 shows the transport critical current densities plotted against susceptibility for a variety of wires, including bare fiber, porous silver, and dense silver cladding of various thicknesses. If one can attribute the volume susceptibility to the fraction of superconducting phase, the interpretation is that the extent of oxygenation (and therefore fraction of superconducting phase) dominates the transport data. This supports the idea that variations in J_c arise from differences in oxygenation.[4]

---

[4]. An alternative reason for the correlation relates to weak link behavior. The susceptibility might not be so simply related to "volume fraction superconductor" for a weak link material, since the measured susceptibility is lowered by weak links. If both J_c and susceptibility are dominated by the severity of the weak links, the correlation provides no useful information.

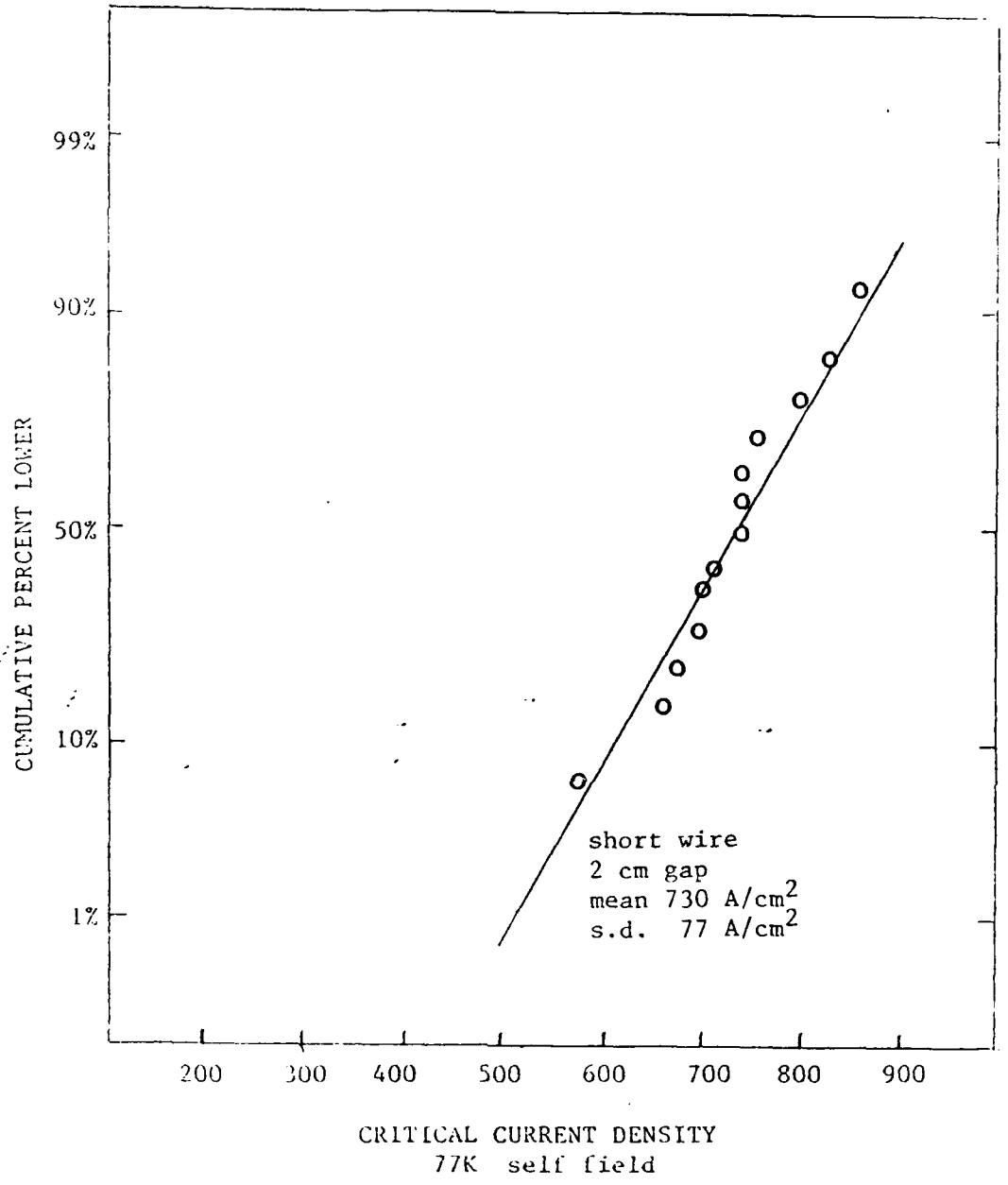

Figure 2.4.1 Distribution of J_c Data for Short Wire Samples

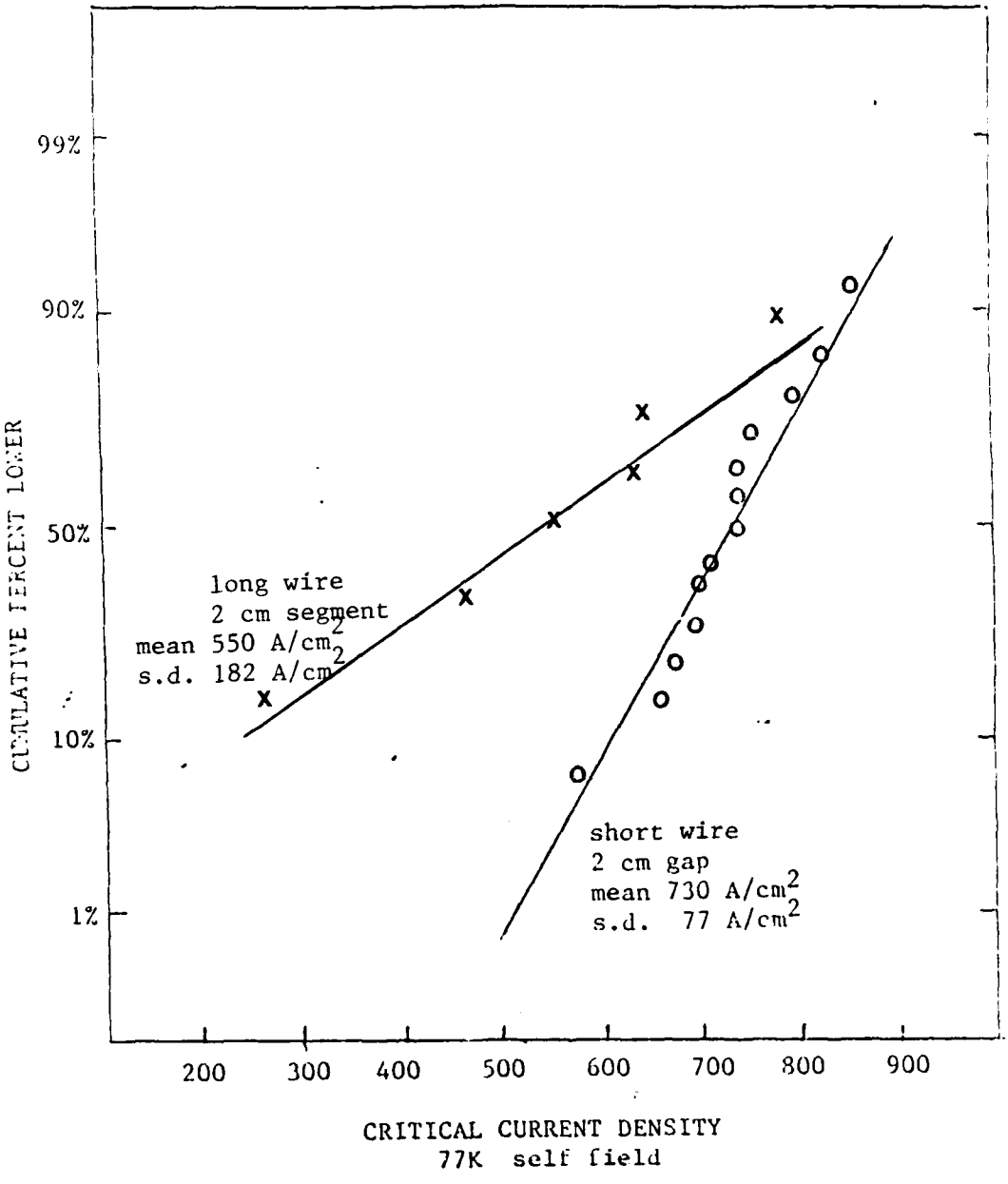

Figure 2.4.2 Distribution of J_c Data for 2-cm Segments of Long Wires Compared with Short Wire Samples at 2-cm Gage Length

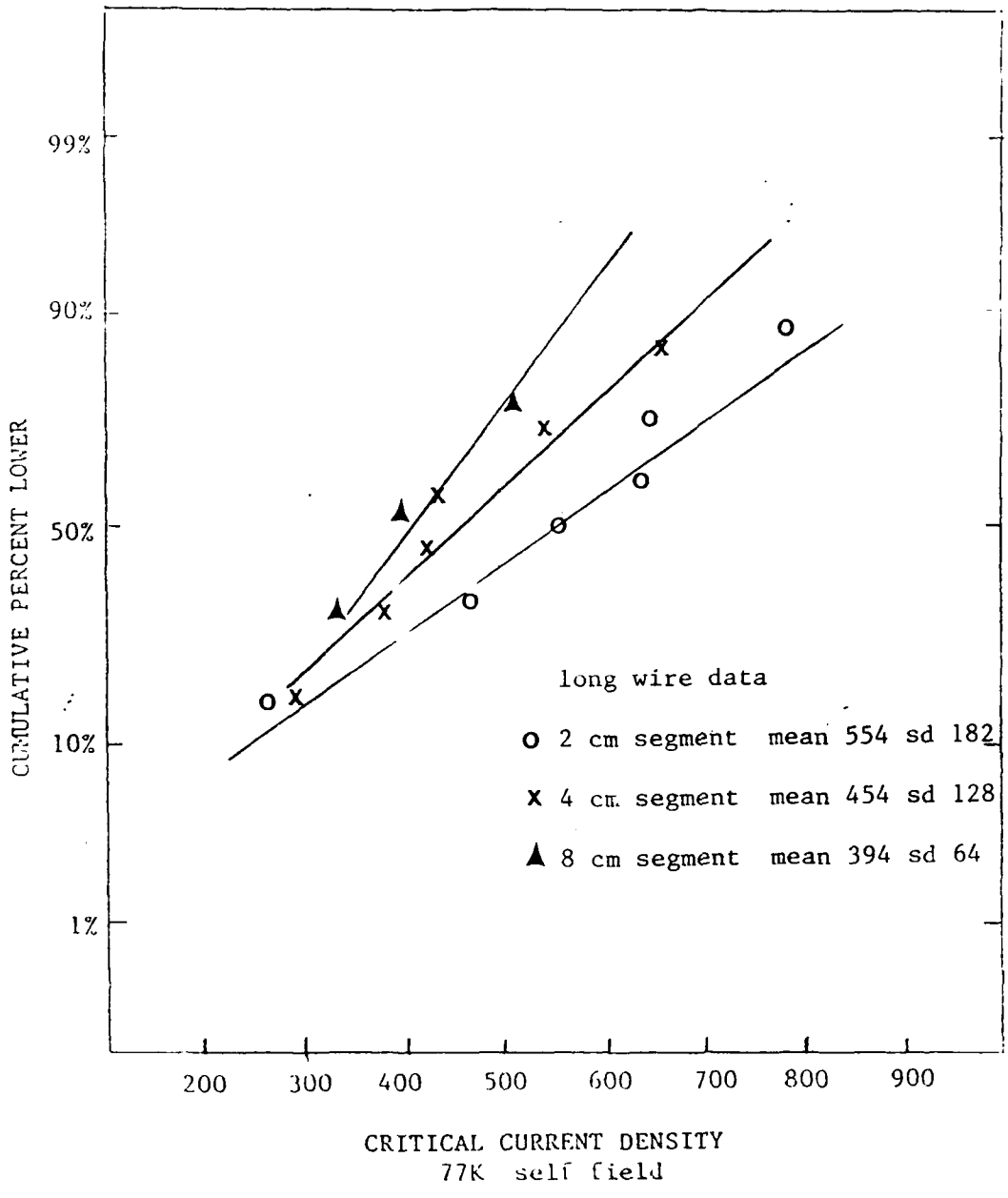

Figure 2.4.3 Distribution of J_c Data for 2-cm Segments, 4- cm Segments, and 8-cm Segments of Long Wires

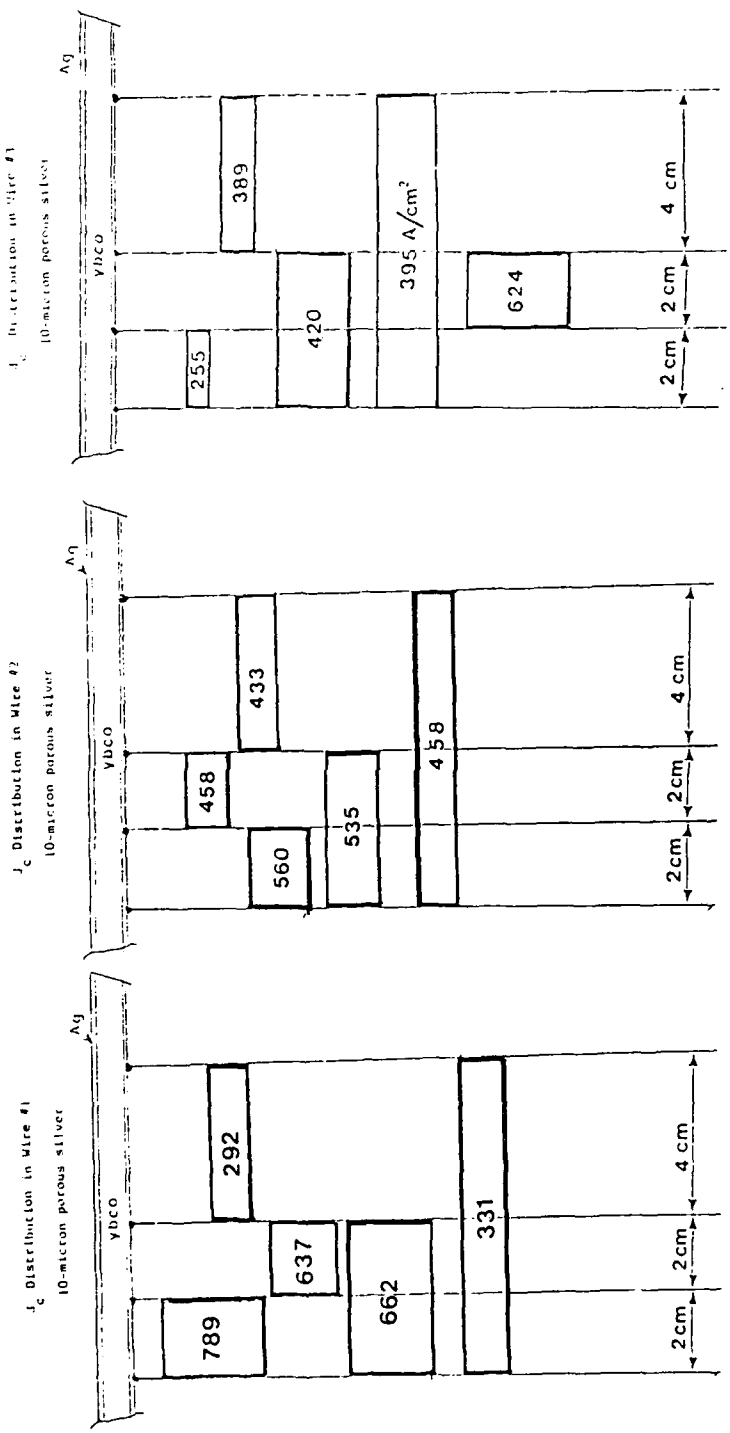

Figure 2.4.4 Spacial Variations of J_c Within Three Long Wires

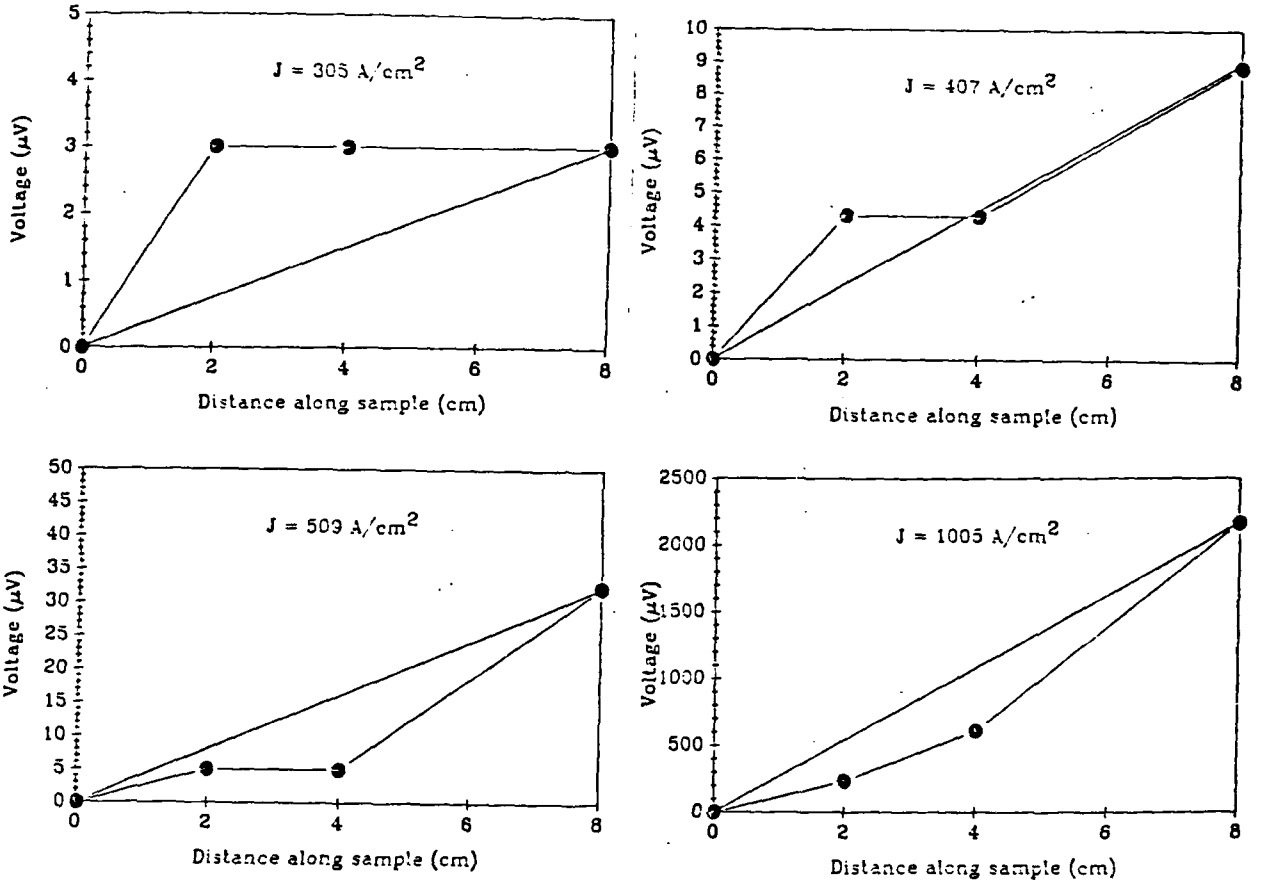

Figure 2.4.5 Voltage Measured at Each of the Four Taps in a Multiple Contact Long Wire at Current Densities of 305-,407-, 509- and 1005 A/cm²

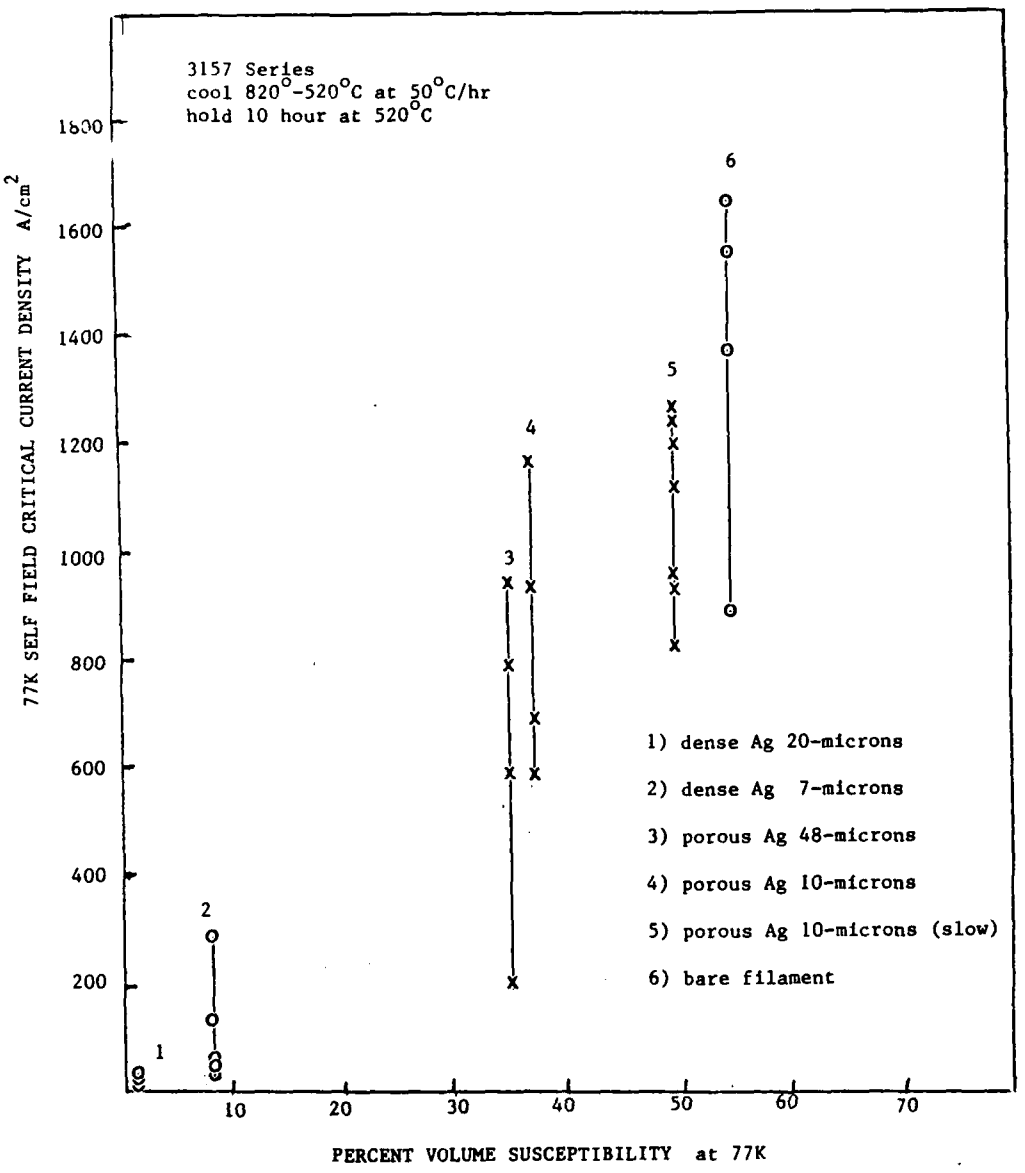

Figure 2.4.6 Transport Critical Current Density vs. Volume Susceptibility at 77K

2.5 Melt Processing of HTSC Wires

The third and most critical stage of Y-123 wire manufacture will be the directional solidification post-process to create a high J_c wire. This was not part of the original project plan, and only recently has the program been restructured to address this issue. Recognizing that melt texturing is the only demonstrated bulk method to make strong-linked Y-123, a major change was made in the contract late last year to focus research on methods to melt texture our Y-123 wire. Resources were reprogrammed from advanced HTSC motor development to materials development to fund new activities aimed at a manufacturing process for high critical current density Y-123 in the form of wire. We had hoped to get these new programs underway during this first quarter of 1990, but this could not be arranged. However, we have preliminary results to report from early exploratory work.

Research will be aimed at melt-texturing YBCO by processes compatible with continuous wire manufacture. Two such methods are presently envisioned: (1) floating zone melting; and (2) metal jacketed zone melting. Floating zone methods rely on surface tension effects to contain a locally heated molten zone. A directionally solidified material is produced by passing the molten zone through a polycrystalline feed rod. As applied to YBCO materials, the floating zone method will convert a sintered feed rod into a melt-textured filament with oriented elongated Y-123 grains. Three variations of floating zone methods will be explored. Laser heated floating zone methods (LFZ) will be explored at ADL, and ORNL will explore floating zone methods using an arc image furnace and a resistive furnace. The floating zone methods will be used primarily to develop compositions and solidification procedures, and not to make wire. While they

are in principal continuous, the work will be done on existing furnaces with limited stroke, which are capable of producing 10-20 cm of directionally solidified material.

Metal jacketed zone melting is a proposed technique for melt texturing a sintered metal clad YBCO wire, with the molten zone contained within the solid metal cladding. Passing the molten zone through the oxide core of the wire creates a composite wire with a directionally solidified YBCO core. This process has the most potential for manufacturing, but must be developed from scratch. Thus we will use the more mature floating zone methods as an experimental method to acquire the necessary solidification information, while doing process development on the metal jacketed technique.

Our goal is make wire, so we eventually must have a zone melting process capable of production rates on the order of a kilometer of wire per day. This is a big challenge, since directional solidification of Y-123 difficult and slow. A key factor influencing the feasibility of manufacturing will be the production rate, which is governed by crystal growth rates. Typically these are in the range of one centimeter per hour. Obviously, practical manufacture will demand an appropriately engineered multi-wire apparatus to obtain viable production rates from an inherently slow process. Our strategy is to simultaneously conduct zone melting at short intervals along the length of the wire. If it is possible for one advancing molten zone to join with the directionally solidified wake of a preceding molten zone, then one can directionally solidify a long wire in a reasonable time. For example, at 1 cm/hour growth rate, one needs to produce a molten zone every 10 cm to directionally solidify the entire wire in 10 hours. A wire one kilometer long requires 10,000 molten zones. We have preliminary designs for an apparatus

which could handle this in a simple and economical fashion.

Our new activities also focus on improving the solidification behavior in the Y-Ba-Cu-O system. Solidification processing of pure Y-123 is complicated by the incongruent melting of Y-123 via the peritectic reaction:

$$2\ YBa_2Cu_3O_7 \rightarrow Y_2BaCuO_5 + (3\ BaCuO_2 + 2\ CuO)_{liquid}$$

which requires that the reformation of Y-123 occur by a liquid-solid reaction. Techniques for controlling this reaction to directionally solidify the Y-123 have been reported[5],[6],[7],[8],[9] although, except for the Hitachi work, the physical form of the material is bulk ingot rather than wire. We are exploring Y-123 alloys away from the 1:2:3 stoichiometry, including Y-123 + Y-211 mixtures, and compositions toward the Y-123 primary crystallization field. We are beginning to investigate a wide range of solidification parameters, including superheat, growth rate, gradient, heat and mass transfer conditions, and the role of atmosphere.

Except for some preliminary work at CPSS using Y-123 pellets for solidification experiments, all of the work used material in the form of fibers or small rods. CPSS will produce all the Y-123 alloys in wire and fiber form. The internal effort at CPS Superconductor is aimed at metal jacketed zone melting of a specially produced SP wire with appropriate YBCO composition and Ag-Pd alloy composition. Melting will be done with a custom built resistively

---

[5] S. Jin et al., Physical Review B, 37,(B), p. 7350-7353, (1988)

[6] M. Mirakami et al., Nippon Steel, Submitted to Japanese J. Applied Physics, (1989)

[7] K. Salama et al., Applied Physics Letters,54, (23) p. 2352-2354 (1989)

[8] M. Okada et al., Hitachi Research Laboratory, paper M7.247, Materials Research Society Meeting, Boston MA, March 29, 1989

[9] E. Yanagisawa et al., op. cit.

heated "microfurnace", capable of producing a small molten zone in a fine HTSC wire. We also focus on metal-ceramic interactions.

Lynn Boatner's group in the Solid State Division at Oak Ridge National Laboratory will supply the resources of a complete crystal growth/solidification group. The program will involve a number of ORNL scientists, with Brian Sales and Brian Chakoumakos as the primary investigators. The major thrust is to identify Y-123 alloys with better solidification behavior, and outline the most favorable solidification conditions. They also will conduct directional solidification experiments on rods and filaments made at CPS Superconductor, using an arc image apparatus and a resistive apparatus, and help develop the metal jacketed approach. The ORNL group also will coordinate all advanced characterization work.

The third leg of this effort is a subcontract at Arthur D. Little on laser float zone (LFZ) processing, led by Edward Peters, one of the pioneers of the LFZ technique. Peters is working closely with CPS Superconductor on laser melting of Y-123 alloy filaments produced at CPS Superconductor. The LFZ wires are being characterized at ADL and CPS Superconductor, with detailed microchemical work to be done at ORNL.

2.5.1 Melt Processing Activities at CPSS

Activities to date at CPSS have been exploratory work examining the melting behavior of YBCO alloys, interactions with the cladding, design and building of prototype equipment. Several versions of the microfurnace have been build and tested. Methods for melting bare fiber and clad fibers have been explored and a series of experiments have been undertaken to reproduce the pellet-style melt texturing work at Nippon Steel. The results will be reported

next quarter.

2.5.2 A. D Little Laser Float Zone Program

This subcontract is not in place yet, but preliminary activities are underway. ADL has demonstrated that they can propagate a floating zone down a 1mm rod of CPS YBCO. About 30 laser floating zone runs have been completed, to begin the exploration of composition and process variables. Figure 2.5.1 is a photograph of several 70% Y-123+ 30% Y-211 rods after the LFZ treatment. The microstructures of the LFZ rods have been characterized at CPSS. Microstructure varies dramatically with LFZ conditions. Figure 2.5.2 shows a polished section of the first LFZ rod, CPS 1, after a post anneal. In the as-grown condition, XRD showed that the rod consisted primarily of barium cuprate and 211, indicating that the cooling rate was too fast for the reverse peritectic reaction. The 211 phase was directionally solidified and located in a central core. In LFZ, the center of the rod is cooler, so the primary crystallizing phase (211 in this case) tends to segregate there. The barium cuprate was found in a thick surface layer. A post-anneal was done in an attempt to reform the Y-123 phase. After 32 hours at 850, XRD showed Y-123 as a major phase, with significant retained barium cuprate and 211 phase. However, comparing the ordinary light with the crossed polarized images of Figure 2.5.2 shows that the Y-123 (bright contrast in crossed polars) grew as fine crystals between the barium cuprate and the directionally solidified 211 core. This points out the need to prevent gross segregation and to do the peritectic anneal more carefully.

We are exploring directional solidification in the primary crystallization field of Y-123. This would promote direct crystallization of Y-123, although

at the primary Y-123 would be combined with a large amount of a eutectic of barium cuprate, CuO, and Y-123. The literature has poor agreement about the location of the Y-123 primary crystallization field, so we undertook a small experiment to establish regions of Y-123 crystallization. We prepared three compositions along the Y-123 -- $BaCuO_2$*CuO join in the psuedobinary shown in Figure 2.5.3. These were prepared from ternary mixtures of Y-123 + $BaCuO_2$ + CuO, formed into a rod, and laser melted. Molten drops were collected in a metal cup where they rapidly solidified. X-ray diffraction showed the presence of Y-123 and barium cuprate, as expected from the phase diagram. We plan to attempt directional solidification by LFZ with these compositions.

CPS #24

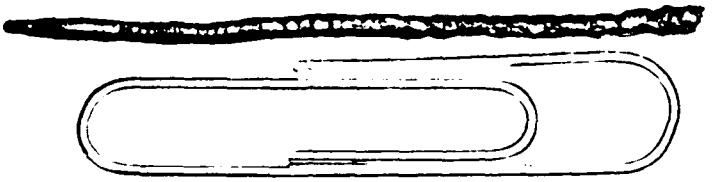

CPS #27

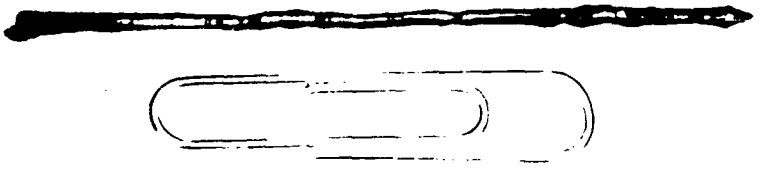

Figure 2.5.1 Laser Float Zone Processed Y-123+Y-211 Rods

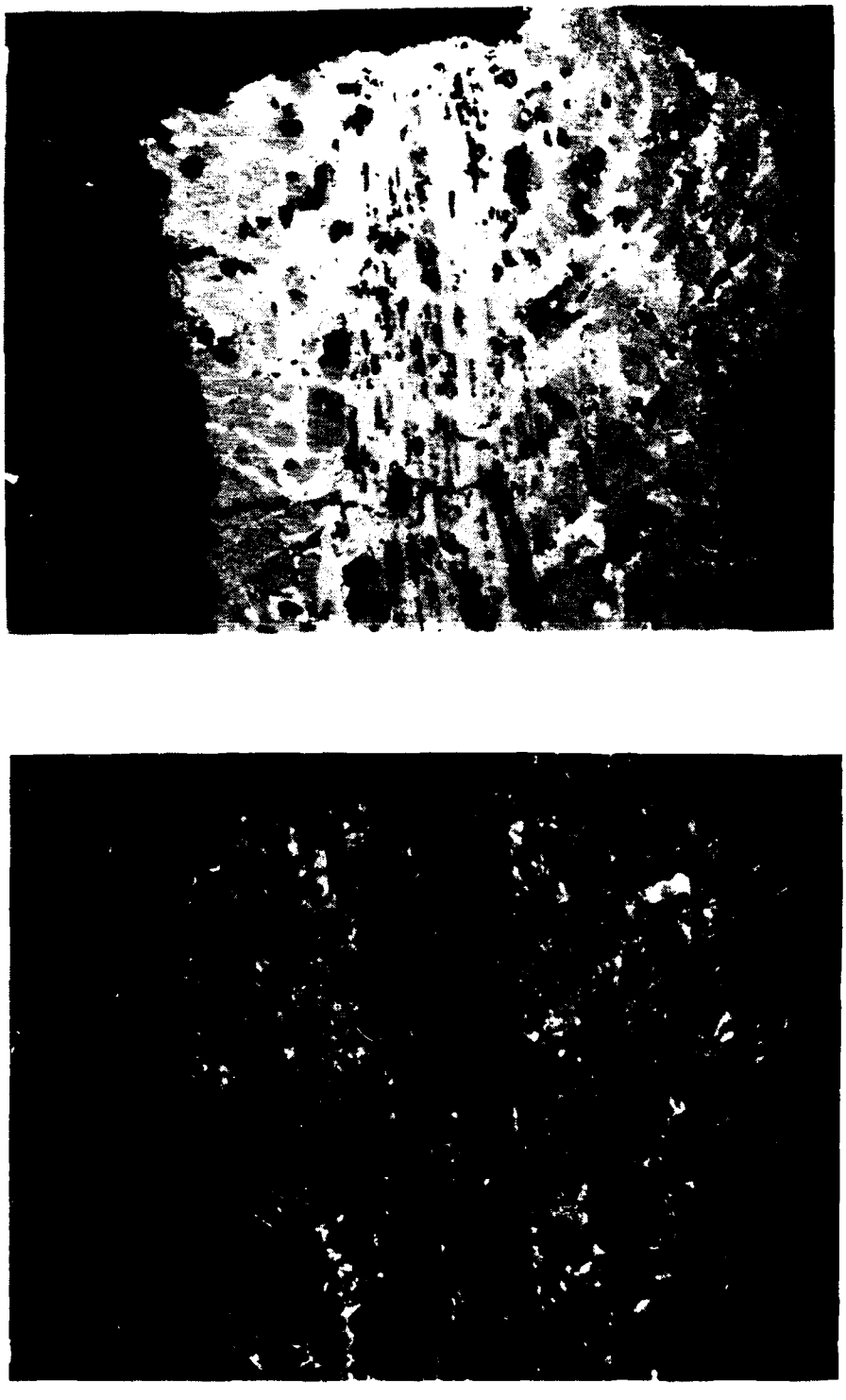

Figure 2.4.2 Polished Section of Laser Float Zone Processed Y-123 Rod CPS-1, after Post-Anneal at 850°C
Above: Ordinary Light Below: Crossed Polars 200X

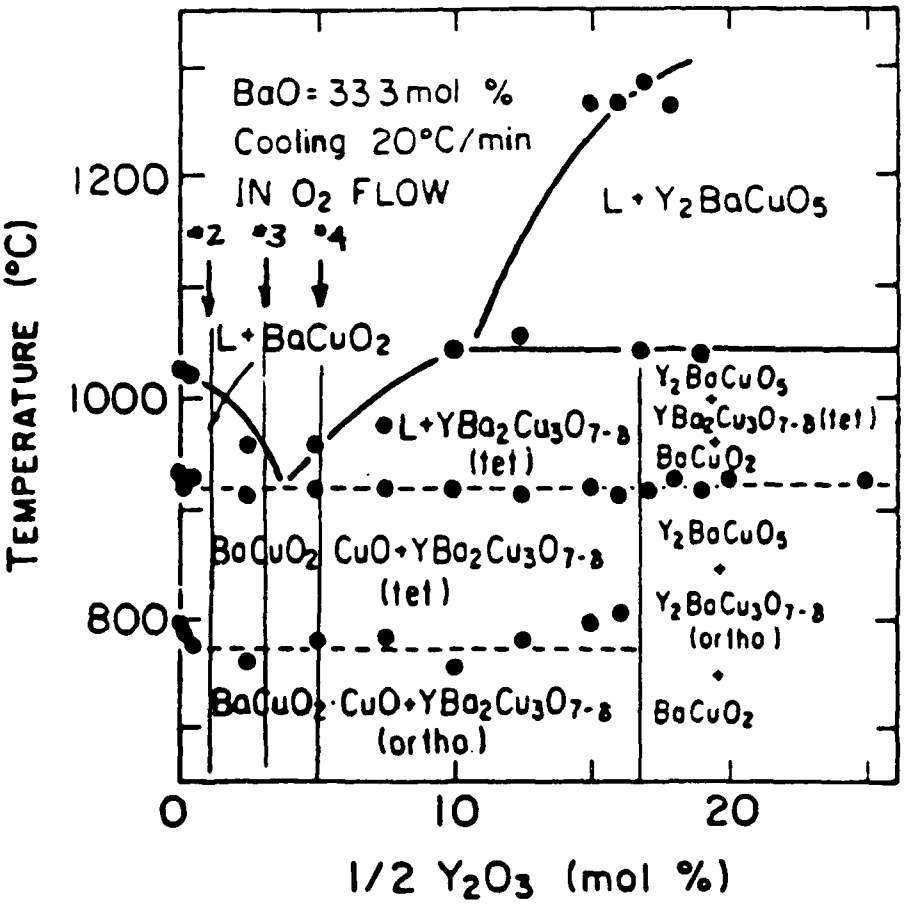

Fig. 8. Pseudo-binary phase diagram for the $YBa_2Cu_3O_{7-\delta}$–$BaCuO_2 \cdot CuO$ system.

Figure 2.5.3 Psuedobinary Diagram for the Y-123 -- $BaCuO_2$+CuO System (After Nomura 1988) Showing Compositions #2,3,and 4

2.5.3 Oak Ridge National Laboratory Pilot Center Program

This subcontract is still being arranged, but preliminary research is already underway, focussing primary on arc image and resistively heated metal jacketed zone melting, using wires supplied by CPS. Results will be presented in the next quarterly report.

2.5.4 Rapid Thermal Processing

We have previously reported briefly on our collaborative work with David Ginley's group at Sandia National Laboratory on rapid thermal processing of HTSC fibers. Rapid Thermal Processing (RTP) uses heat treatments of 2-4 sec. around 1000°C with a 3 min. cool down in oxygen to densify (burned out) green fiber or oxygenated presintered fibers. Rapid thermal processing rapidly densifies unsintered material, creating a microstructure characteristic of the fiber composition, RTP temperature and time. Green fibers are rapidly densified, displaying microstructures characterized by large grains with distinctive blocky or elongated morphology. Presintered Y-123 fibers do not undergo drastic microstructural change after RTP, but are rapidly oxygenated by the treatment.

Of particular interest is the fact that RTP annealed Y-123 is superconducting immediately after the RTP anneal, without requiring the 500°C oxygen anneal which is conventional for Y-123. Indeed, conventionally sintered Y-123 fibers, which are semiconducting in their as-sintered state, become superconducting after an RTP treatment, indicating that very rapid oxygenation occurs during RTP. Experiments with RTP of tetragonal Y-123 fibers made by pre-sintering in N_2 show that re-oxygenation by RTP in oxygen occurs during the 1-4 second isothermal hold at 1000°C, rather than during the 3-minute cooling

ramp. Twinned orthorhombic Y-123 grows predominantly from grain boundaries, suggesting grain boundary diffusion of oxygen during the RTP anneal.

RTP has produced Y-123 material having, at best, similar properties to conventionally sintered Y-123 fibers, with $T_{c,r=0}$ of up to 90K and self field J_c to 1200 A/cm^2. To date, all RTP specimens have been weak-linked. We are continuing to explore the technique and, with NASA funding[10], are exploring RTP of continuous wires.1

Appended to this report is a paper in which we discuss in more detail the development of the microstructure when sintering occurs by RTP and characterize the phenomenon of rapid oxygenation by examining superconducting properties of pre-sintered Y-123 after RTP treatment.

---

[10]NASA-Lewis Research Center SBIR contract NAS 3-25876

SECTION 3

HIGH TEMPERATURE SUPERCONDUCTOR MOTOR DESIGN AND FABRICATION

ALAN CRAPO AND JERRY LLOYD

EMERSON MOTOR COMPANY

MOHAMED HILAL

UNIVERSITY OF WISCONSIN

3.1 Introduction

The major activities this quarter have been in the areas of increasing the torque output of the HTSC homopolar motor, getting the homopolar motor built, and analyzing advanced motor designs with future HTSC wire properties. To increase torque output, a design using multiple bobbins for non-uniform current distribution was investigated. The motor construction status is also updated in the report. We have been evaluating advanced, high performance HTSC motor designs in terms of future wire properties and potential applications. We have been looking at high performance homopolar DC and heteropolar DC motors. We have gone into more depth investigating an HTSC brushless DC motor. The results are presented in this report.

3.2 Homopolar Motor Design Enhancements

HTSC wire properties of today are not as good as we had hoped when we first designed the homopolar motor. Lower current densities in a magnetic

field mean less torque out of the motor. In order to increase the torque of the present designs, we have made some minor modifications to the design.

Last quarter, we reported that when we incorporated today's HTSC wire properties into the design of the Homopolar DC motor, we would theoretically only be able to get 25% of the originally designed field due to the critical current density being reduced severely by the magnetic field. We designed the field winding for a current density of 1000 Amperes/cm^2 in a field of 100 Gauss. This corresponds to a current of 0.125 Amperes in the 4600 turn coil producing a worst case field of 100 Gauss at the ends of the coil producing 976 Watts of output power at 3000 RPM. The wire can actually carry over 2000 Amperes/cm^2 in a 0 Gauss field, but can only carry 30 Amperes/cm^2 in a 100 Gauss field. The Motor design characteristics and the wire properties give 250 Amperes/cm^2 in a worst case 25 Gauss field. This results in 84 Watts of output power at 3000 RPM which is 9% of the original design level.

Since only the ends of the coil are at the maximum flux density, we can theoretically operate at a higher current density in the middle of the coil and get more total Ampere-turns than with one single coil. Figure 3.2.1 shows the cross section of six small wound bobbins on the large bobbin. Figure 3.2.2 shows the current density versus magnetic field for the HTSC wire. Since the magnetic field is lower in the middle of the coil, we can increase the current in those sections, resulting in more total ampere turns. Figure 3.2.3 shows the current density and flux density distribution of the coil divided into six smaller coils, each with separate excitation, optimized for maximum total Ampere turns.

This approach can theoretically give us a 21% increase in field over a uniform current density configuration. This increases the shaft power to

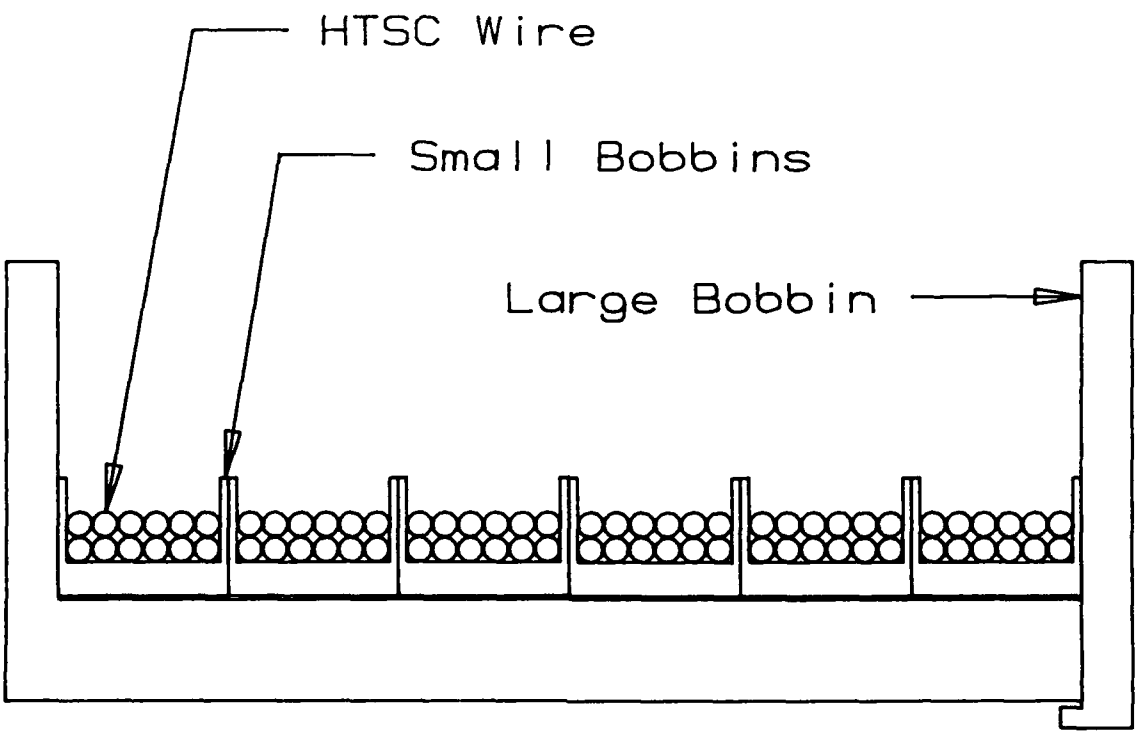

Figure 3.2.1 Cross Section of
Six Small Bobbins on Large Bobbin

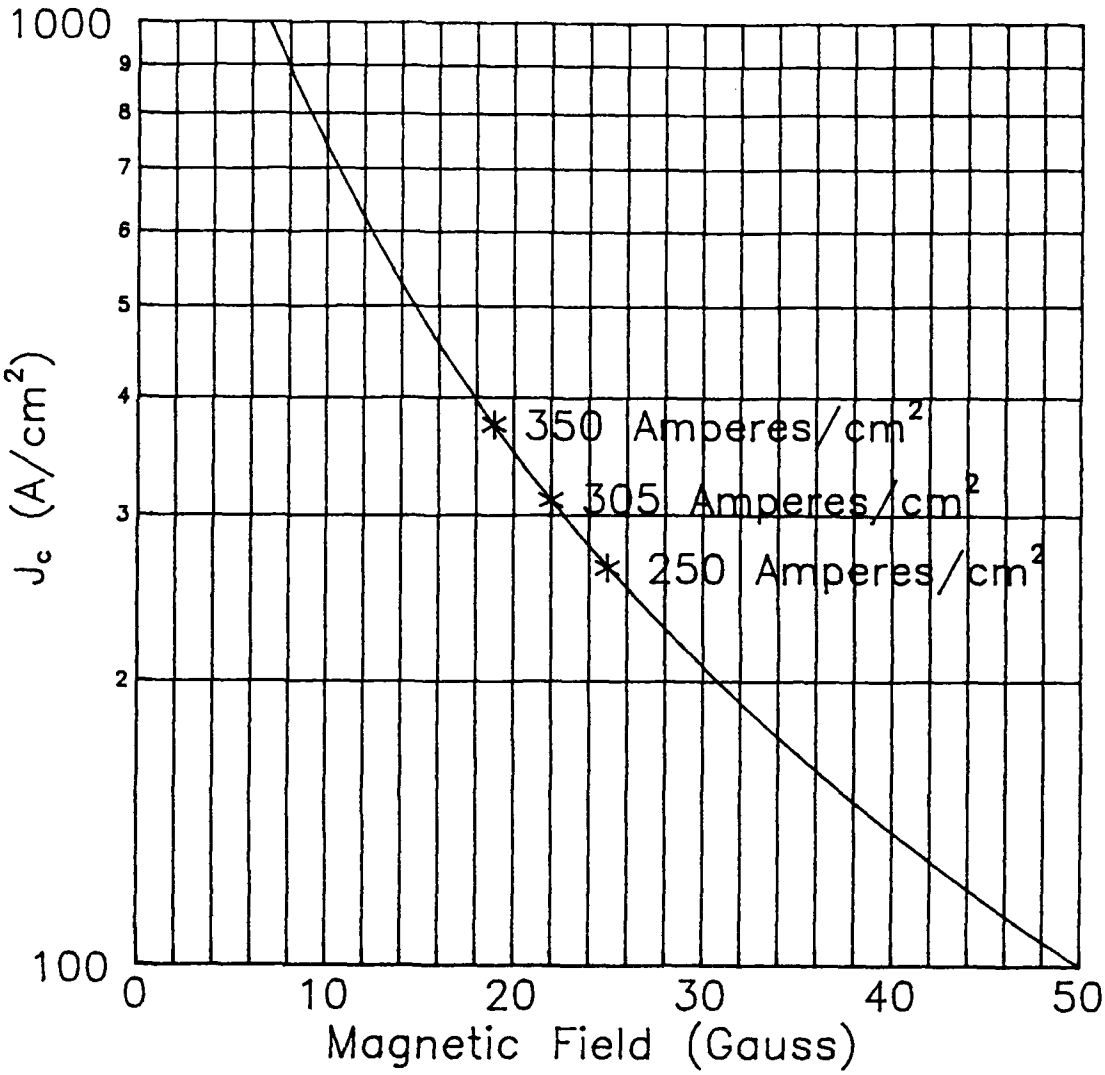

* Coil Operating Points

Figure 3.2.2 Current Density Versus Magnetic Field for HTSC Wire.

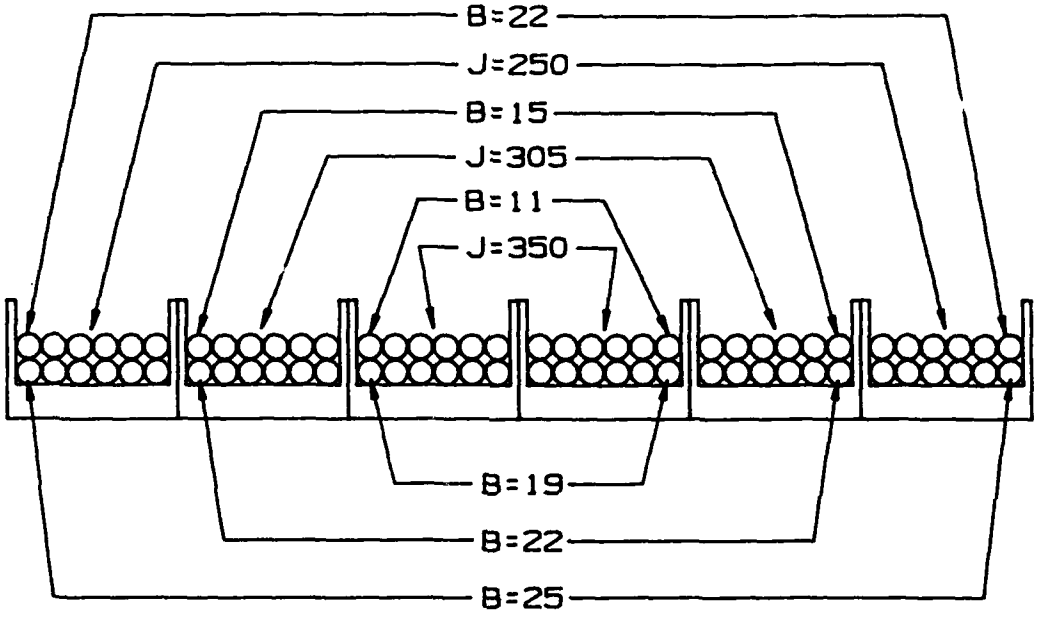

Flux Densities(B) in Gauss
Current Densities(J) in Amperes/cm²

Figure 3.2.3 Flux Densities and Current Densities in Six Small HTSC Coils with Optimized Current Distribution

150 Watts at 3000 RPM which is a 79% improvement over the single coil version, and brings us up to 15% of the original designed shaft output power. In actuality, we may be able to get even better improvement. Each coil is limited by its weakest section. Smaller coils reduce the likelihood of a really bad section. Since no two coils will be the same, we can characterize the coils and optimally place them for maximum current density in a magnetic field.

Another major advantage of this approach is that CPS will be making 767 turn coils instead of 4600 turn coils. In a practical sense, the smaller coils are less difficult to handle and can be made in shorter "intensive labor" periods. This will also give us the option of changing out any coils that are bad or damaged without destroying the other coils.

3.3 Homopolar Motor Construction

Motor construction is coming along well. Most of the parts are done. The above design improvements have slowed things a little, but will substantially improve the motor. All of the test equipment is ready. Bobbins have been wound with copper wire, and we are currently building the first motor with copper coils. This will give us a performance baseline and some experience with the motor before we put HTSC coils in. We will be able to measure motor performance as a function of field current. We will also be able to iron out any bugs in the motor both at room temperature and in liquid nitrogen before the HTSC coils are installed.

3.4 Advanced HTSC Motor Designs.

As HTSC wire properties improve, Advance high performance superconductor motors will become possible. We are continually looking at possible motor designs to best take advantage of new wire properties as they become available. We are also looking at what current densities in a magnetic field are necessary for a viable motor in the various designs. Eventually, we would like to focus the advanced HTSC motor designs on the 50 horsepower size.

3.4.1 High Performance Homopolar DC Motor

The Homopolar DC motor is still an attractive design for ship propulsion or other large scale applications where high current low voltage power is available. They are well suited to superconductor field windings because of the absence of AC fields and currents. When high current and low voltage is not available, as in industrial applications, Homopolar DC motors are probably not the best choice. High voltage, low current versions of homopolar motors tend to be large and not as efficient as other motor designs. Any 50 horsepower HTSC Homopolar DC motor would probably be a prototype of a large machine for heavy power applications.

3.4.2 Heteropolar DC Motor

For applications with high voltage input power requirements, Heteropolar DC motors are an alternative. In the third quarterly report and the first annual report, we discussed a heteropolar DC motor with HTSC field windings to produce up to 3 Tesla in the air gap with no steel in the magnetic circuit but the design still used conventional copper windings in the armature. This design had some advantages over a conventional motor but did

not have a huge increase in the power density. We will be considering a version which not only has HTSC field windings, but HTSC armature windings. This "all HTSC" version will have much higher power density. The results will be presented in the next report.

3.4.3 Brushless HTSC "Permanent Magnet"

The concept of trapping flux in a superconductor coil or in bulk material to make a super high energy "permanent magnet" is a fascinating one. As the flux trapping capability of HTSC materials improves, this concept can become a reality for motor applications. In theory, these magnets could be five to ten time higher energy than conventional rare earth magnets of today.

Just as conventional permanent magnets need to be magnetized, HTSC coils or bulk material needs to be "charged" or "magnetized". A magnetic field is applied while the superconductor is above the critical temperature, and then the superconductor is cooled below the critical temperature. When the field excitation is removed, currents in the superconductor will circulate to maintain the field and keep it from decaying. In a brushless motor, this would be done by having superconducting stator windings in a cryostat, and a rotor with a superconducting ring or coils in its own cryostat. The stator would be cooled and high DC currents would be put through the superconducting windings while the rotor was still above the critical temperature. The rotor would then be cooled to trap the flux. The rotor would then act much like a permanent magnet rotor.

To analyze the performance of the motor design, finite element magnetic field modeling was used. A stator frame that is 11 inches in diameter and an axial length of active material of 5 inches was modeled.

Figure 3.4.1 shows 1/6 of a six pole motor while the stator is supplying flux to the rotor. The HTSC winding is operating at a current density of 100,000 Amperes/cm^2 in a 2.0 Tesla field, with 20% of the coil space consisting of HTSC material. This produces a peak field of 1.0 Tesla on the surface of the rotor. When the stator field is removed, Figure 3.4.2 shows the same flux at rotor surface. Figure 3.4.3 shows the rotor flux combined with the stator flux in the peak torque position. The current density in the HTSC stator winding is again 100,000 Amperes/cm^2 with 20 % of the coil volume consisting of HTSC material. The peak flux density in the coil is 2.0 Tesla. The peak flux density in the air gap is 2.4 Tesla. The torque calculated for these conditions is 2439 Newton meters. At 1800 RPM that would be 616 horsepower.

Even though this motor could theoretically produce 2439 Newton meters of torque, the practical mechanical aspects of the design would limit the torque to a much lower value. The sheer strength of materials would limit the safe output to around 100 horsepower or less at 1800 RPM.

For comparison, an induction motor of the same size in a totally enclosed fan cooled 284T frame is 15 horsepower at 1770 RPM with a service factor of 1.25. The maximum continuous rating is 18.75 horsepower. A brushless rare earth permanent magnet motor using samarium cobalt or neodymium-iron-boron magnets in the same package size can produce 180 Newton meters of torque at 1800 RPM or 45.5 horsepower in the same package size.

The torque of the HTSC DC brushless motor will vary with the stator current density squared. The rotor flux is proportional to the stator flux and the torque is proportional to the product of the two fluxes. The torque in Newton meters, and the horsepower at 1800 RPM are given by:

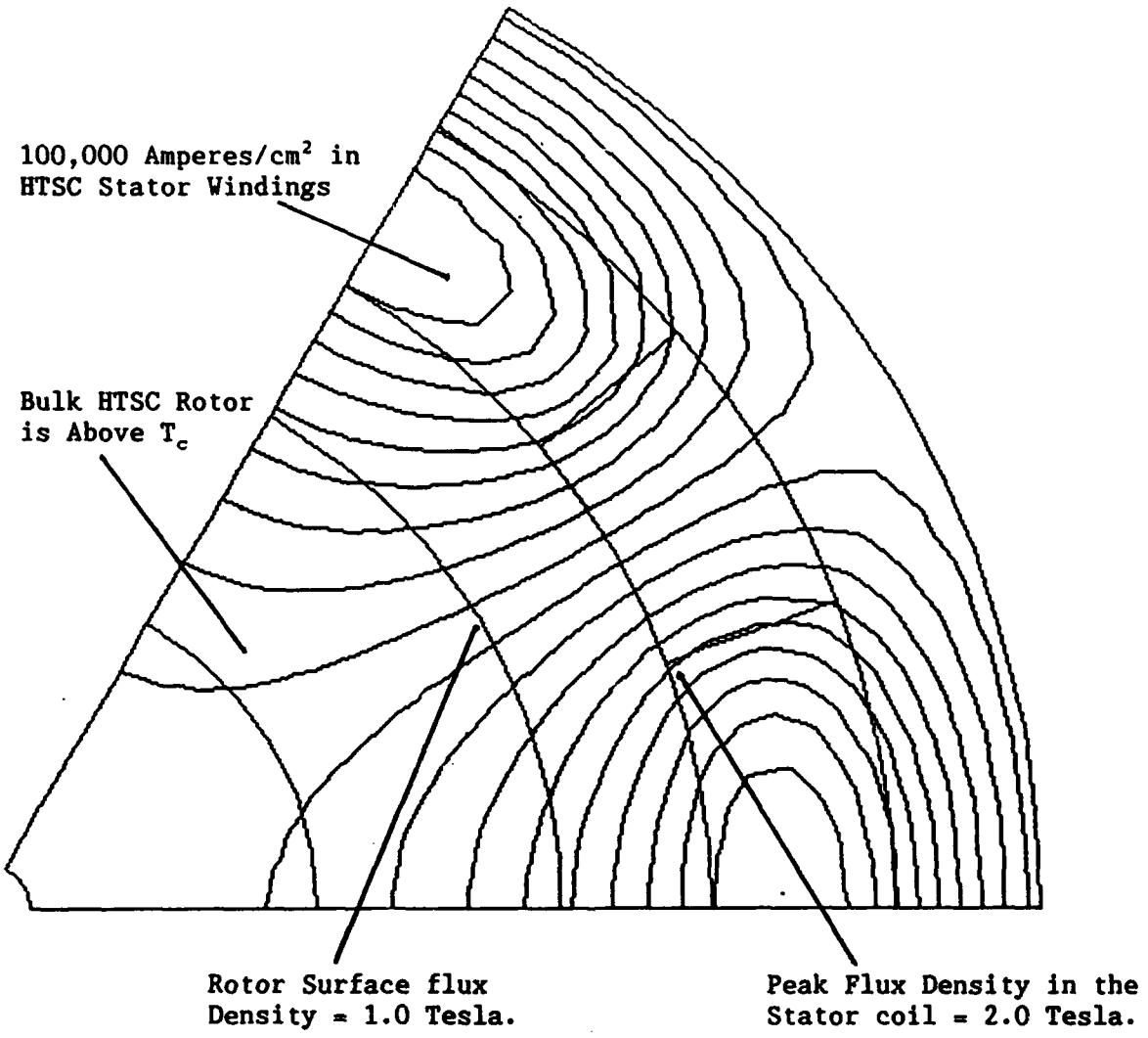

Figure 3.4.1 HTSC Stator Supplies magnetic Field to charge the Rotor of a Superconductor Brushless DC motor.

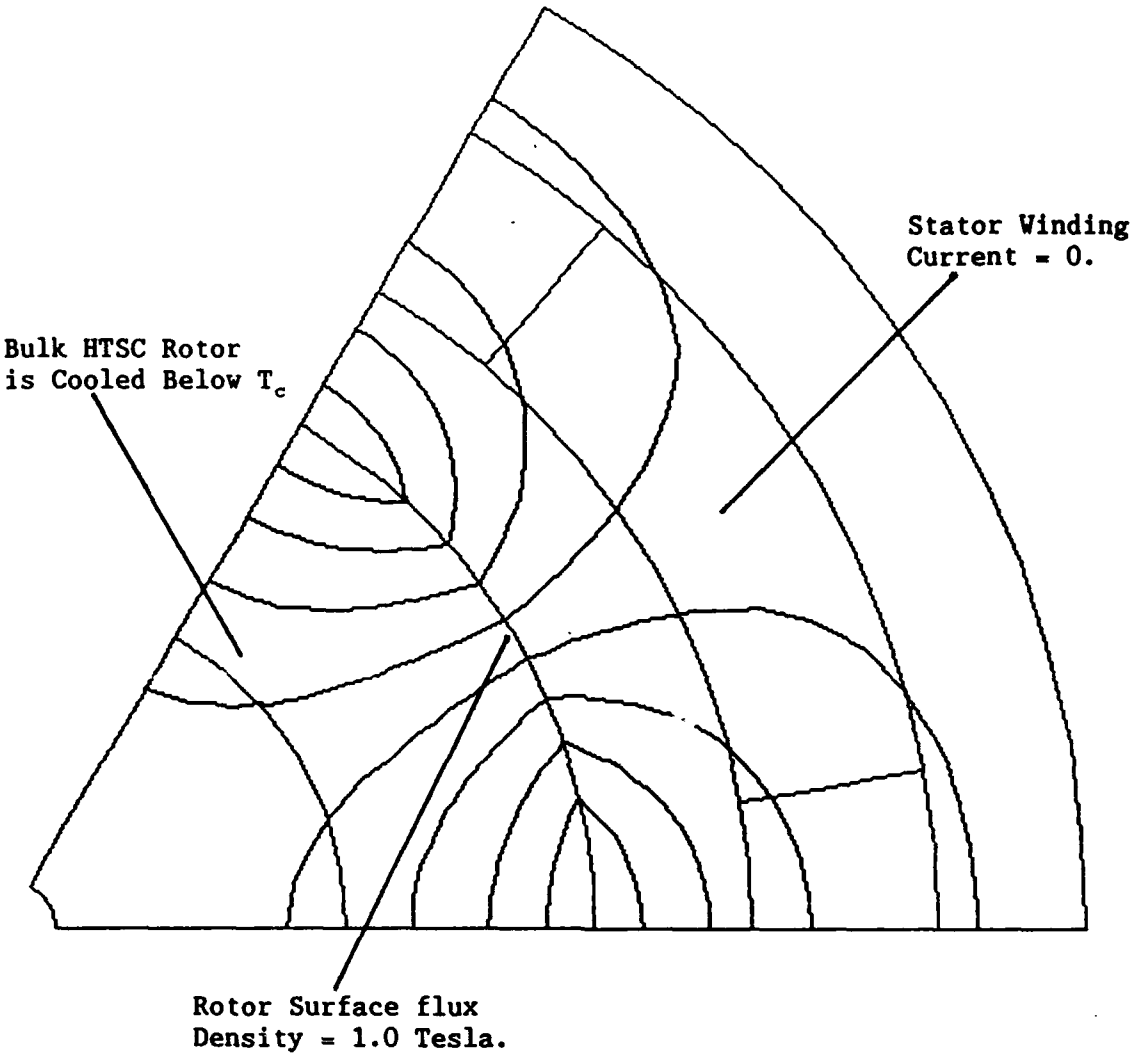

Figure 3.4.2 Flux is Trapped in the HTSC Material After the Rotor is Cooled in a Magnetic Field.

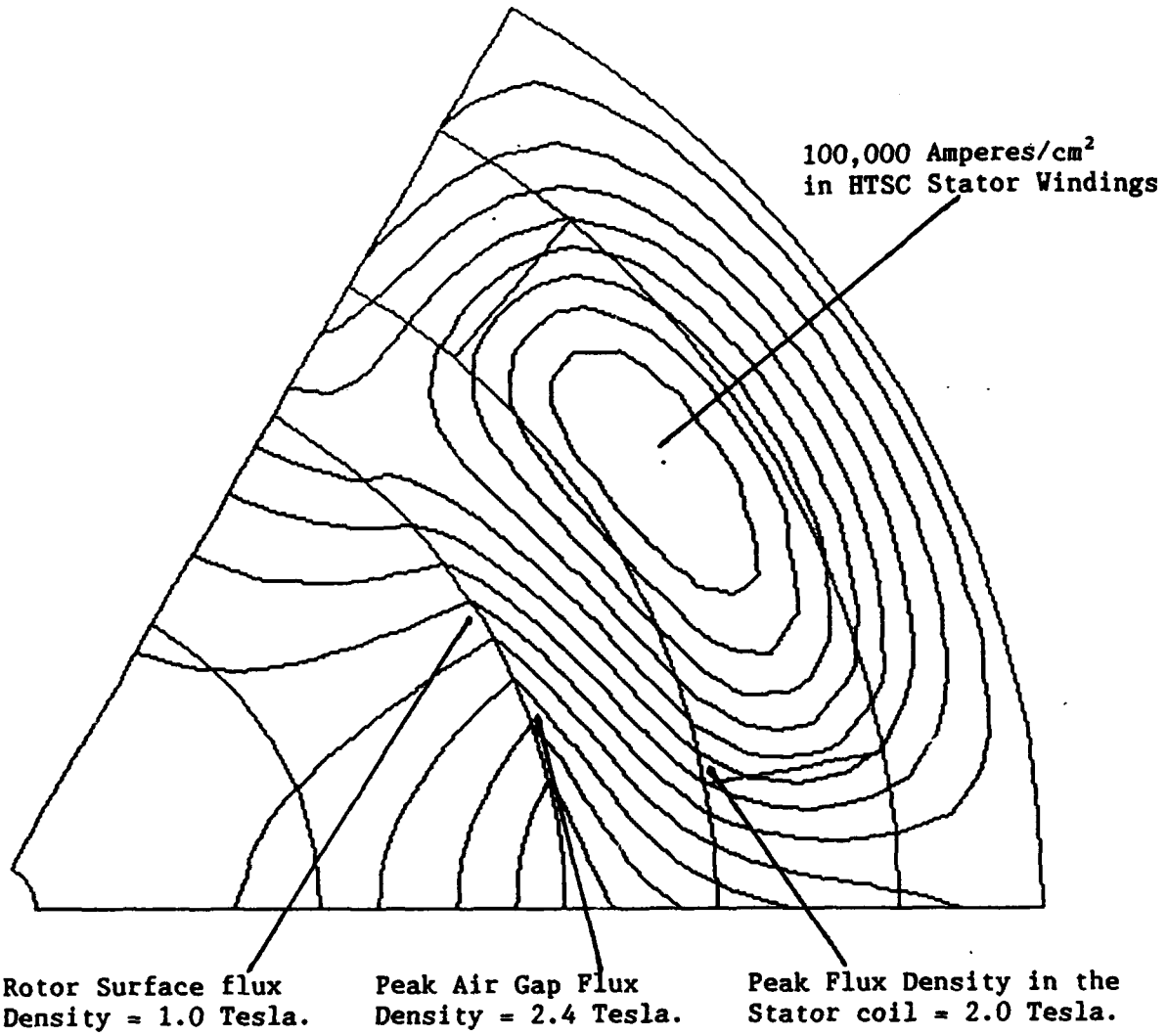

Figure 3.4.3 HTSC Brushless DC Rotor Flux and Stator Flux Combine in the Peak Torque Position.

Torque = $2.439 \times 10^{-7} J^2$

Horsepower at 1800 RPM = $6.163 \times 10^{-8} J^2$

Where : J is the current density in Amperes/cm^2

Figure 3.4.4 shows the horsepower versus current density for this motor design. For low current density, the power output is very low. A current density of 34,000 Amperes/cm^2 with a peak coil flux density of 0.54 Tesla would produce 45.5 horsepower like the rare earth brushless DC motor. In order to produce 18.75 horsepower like the induction motor, the HTSC brushless DC motor would need 22,000 Amperes/cm^2 in a peak field of 0.35 Tesla.

These comparisons apply for the brushless DC motor design presented here. Next quarter, we will continue to analyze other motor design concepts. We will look at power outputs and current densities necessary to make the designs viable.

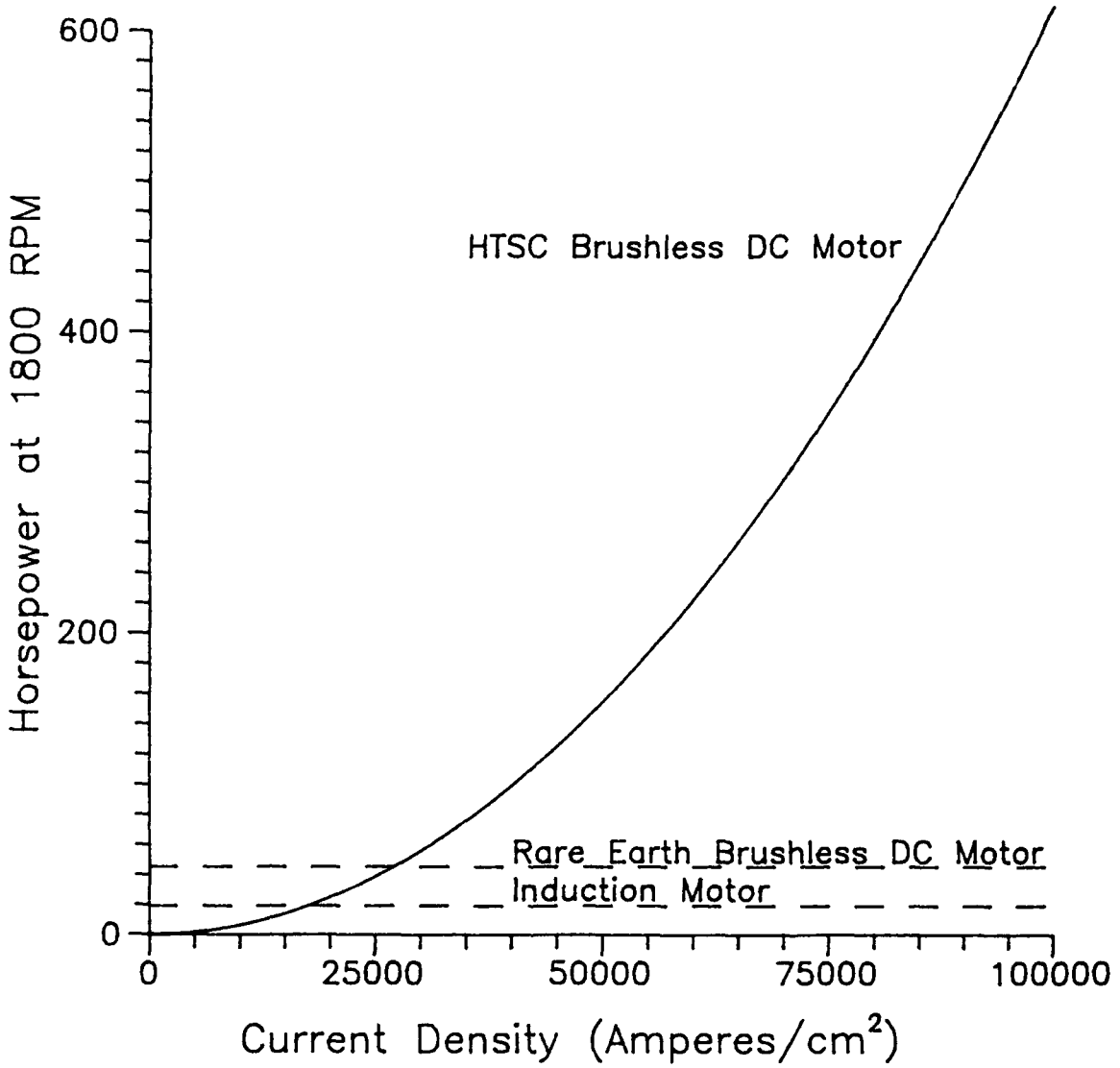

Figure 3.4.4 Horsepower versus Current Density in HTSC Stator Windings.

SECTION 4

GENERAL DISCUSSION AND SUMMARY

SUMMARY

We are significantly closer to both of our project goals. The homopolar motor will soon be ready to test with HTSC field coils, and the HTSC wire will, after scale-up, be ready to wind the field coils. Both activities are confronting the present availability of low J_c weak link wire, and the considering the options for producing and designing with high J_c wire.

The major activity in wire development was a scale-up of the process for fabricating silver clad polycrystalline Y-123 wire, but we also began to expand development of BiSCCO and melt textured Y-123. This research aims for a three-step process wire manufacturing process involving: (1) preparation of "green clad" fiber; (2) continuously sintering to produce silver-clad sintered polycrystalline wire (SP wire), and (3) post-processing to make a high critical current density wire. The first two steps have been demonstrated and now are being scaled-up to provide the six kilometers of wire required to fabricate two 575 ampere-turn field coils for the Emerson homopolar motor. Each coil is made from six segments wound with 500 meters of wire. This quarter we produced more than 166 meters of sintered polycrystalline Y-123 wire, some of which was wound onto Emerson homopolar motor coil bobbins.

We increased develop efforts on post-processing of sintered Y-123 wire directional crystallization. In parallel development to produce sintered wire from the Bi(Pb)SCCO systems, we have determined the powder production and sintering conditions giving fabricat[illegible] tapes with zero resistance at 108K.

Green fiber, green clad wire, and sintered polycrystalline wire has been produced from the BiSCCO material, and we have demonstrated that the silver-clad sintered wire can be cold rolled into a tape.

We completed the extension to our sintering furnace, and now have in place a process in which spools of green clad fiber are fed into the belt furnace and collected as spools of sintered clad wire at the furnace exit. We have made steady progress toward continuous uninterrupted furnace operation. By identifying and solving a series of practical problems, we have been able to run up to 13 hours without a wire-breaking incident. We are developing annealing procedures for long wires, which will be batch annealed as coils of sintered wire. A high temperature alloy annealing retort has been designed and fabricated.

Melt texturing research work involved static furnace anneals of pellets and fibers at CPS exploring a range of YBCO compositions and Ag-Pd coatings. Preliminary experiments were done in preparation for the upcoming subcontracts at A.D. Little and Oak Ridge National Laboratory aimed at melt processing of wires and fibers. Also, work continued in collaboration with Sandia and Los Alamos National Laboratories on rapid thermal processing of Y-123, with most emphasis on characterizing the rapid oxygenation effect.

The design of the HTSC homopolar motor has been improved. In a effort to increase the output from field coils made with weak-linked wire, we redesigned the field winding. The single coil was replaced with six smaller coils energized with three independent circuits so the current could be separately controlled. By separately optimizing the current in each coil, we can obtain a 79% improvement over the single coil version. Motor construction is in progress, with the first prototype wound with copper coils. The copper coils

will be used to debug the machine before the HTSC coils are installed.

Preliminary design is underway on two new HTSC motors, which would be more advantageous over homopolar in low current environments. For applications with high voltage input power requirements, a heteropolar DC machine with HTSC field windings and armature is being considered. The second machine is a brushless permanent magnet DC motor, in which the "permanent magnet" field is produced by trapped flux in an HTSC rotor. If trapped flux density can be as large as 2 T, such a machine could have a horsepower output 30 times greater than an induction motor of similar size and more than 10 times greater than a conventional permanent magnet motor.

APPENDIX A

Spring MRS Meeting

RAPID THERMAL PROCESSING OF HIGH TEMPERATURE SUPERCONDUCTING FIBER

J.W. HALLORAN*, M.J. NEAL*, D.S.GINLEY**, E.L. VENTURINI**, J.F. KWAK**, R.J. BAUGHMAN**,M.A. MITCHELL**,B.MOROSIN**,S.N. BASU*** and T.E. MITCHELL***

*CPS Superconductor Corporation, Milford, MA 01757 **Sandia National Laboratories, Albuquerque, NM 87185 ***Los Alamos National Laboratories, Los Alamos, NM 87545

Abstract

We report on the rapid thermal processing (RTP) of $YBa_2Cu_3O_7$ (Y-123) fibers. Unsintered fibers are densified by RTP. We show that fibers which were originally semiconducting and tetragonal before RTP form normal twinned orthorhombic material after processing for 2-4 seconds above 1000°C with a 3 min. cool down in oxygen. They subsequently show T_c to 90K and magnetization indicative of substantially shielding. We present the effects of varying the RTP parameters on the morphology, phase, and superconducting properties of a number of tetragonal and orthorhombic Y-123 fibers.

Introduction

We have previously reported that Rapid Thermal Processing (RTP), using heat treatments as short as one second at temperatures around 1000°C, is an effective processing technique for high temperature superconductors [1,2]. RTP of $YBa_2Cu_3O_7$ (Y-123) fibers has produced material with $T_{c,r=0}$ of up to 90K and self field J_c to 1200 A/cm^2. RTP rapidly densifies unsintered material, creating a microstructure characteristic of the fiber composition, RTP temperature and time. Of particular interest is the fact that RTP annealed Y-123 is superconducting immediately after the RTP anneal, without requiring the 500°C oxygen anneal which is conventional for Y-123. Indeed, conventionally sintered Y-123 fibers, which are semiconducting in their as-sintered state, become superconducting after an RTP treatment, indicating that very rapid oxygenation occurs during RTP.

In this paper we discuss the development of the microstructure when sintering occurs by RTP and characterize the phenomenon of rapid oxygenation by examining superconducting properties of pre-sintered Y-123 after RTP treatment.

EXPERIMENTAL PROCEDURE

Fabrication of Fibers

Fibers were produced using a proprietary process in which Y-123 powders are compounded with a thermoplastic resin so they can be spun into continuous "green" fibers using a conventional textile fiber spinning machine. Most fibers used in this study had a green diameter of 125 microns. The powder was a phase pure Y-123 with 1.6 micron average particle diameter. Copper oxide-rich fibers were prepared with a 5 wt% admixture of CuO. Fibers which were RTP annealed in the unfired state had undergone a binder burnout in which the fibers were heated in air at 20°C/minute to 500°C, held for 10 minutes, then cooled to room temperature at 10°C/minute. This treatment removes most of the organic material, but does not allow any sintering of the Y-123. Pre-sintered fibers received a binder burnout and a 945°C/30 min sintering anneal in a continuous furnace, yielding a sintered density about 90% of theoretical.

Rapid Thermal Processing

Burned-out unsintered fibers and presintered fibers were RTP annealed in an ADDAX-AET model R-1000 rapid thermal annealer. The fibers were supported on a 4" Si wafer coated with 1 micron of silicon nitride. The system was equipped with two low mass thermocouples with one or both in direct contact with the fibers. Before during each run the system (100 cc chamber volume) was purged with high purity oxygen at 3 liters/sec. Typical run conditions (all under 1 atm. oxygen) were: i) a 10 second wait period, ii) 4 second ramp to peak temperature, iii) hold at peak temperature 1-4 seconds, iv) cooling ramp to 600°C

in 96 seconds, v) ramp to room temperature in 180 seconds. The programmed measured temperature agreed within 1%, except when below 300°C where the actual cooling rate lagged the program. The coated Si wafer was an effective substrate in cases reported here, with no apparent reaction with the fibers during the brief RTP anneal. At higher temperature, fibers reacted with the substrate.

Characterization

After RTP, specimens were characterized in the as-fired condition, with no oxygen anneal. Oxygen anneals, though not discussed here, did improve the superconducting properties in some cases. Fibers were examined by X-ray diffractometry had patterns indicative of well formed orthorhombic Y-123, although in some cases the lines were not as sharp as our best material. Precession photographs indicated no preferred orientation. The microstructures were characterized by optical microscopy, scanning electron microscopy, and transmission electron microscopy. Transport properties were determined with standard 4-probe techniques. Magnetization measurements down to 5K were performed in a SQUID magnetometer at 100 Oe, and AC susceptibility at 10 Oe was measured down to 75K.

RESULTS

Microstructure Development

Green Y-123 fibers sintered by RTP develop a sequence of microstructures depending upon time, temperature, and composition. It was generally observed that very rapid grain growth, suggestive of liquid phase formation, occurred in a narrow +/-25°C temperature window. Below the window there is local sintering of grains into dense patches, but no grain growth so the grain size remains 1-2 microns. As the window is approached, rapid grain growth creates distinctive blocky grains as large as 10 microns. At higher temperature, there is a profound change in grain morphology, creating locally oriented patches of elongated grains as large as 50 microns. Figure 1 is a series of SEM micrographs illustrating the evolution of microstructure with temperature and time for Y-123+5% CuO fibers. Figure 1A illustrates the fracture surface after a 1025°C/2 sec RTP anneal at, showing the blocky grain morphology. This microstructure is uniform throughout the cross-section of the fiber. A 4-sec RTP anneal at the same temperature creates the elongated grain structure shown in Figure 1B. Lower magnification views of this specimen, not shown here, show that the elongated grains form in circular patches with the grains radiating from a central nucleus. This suggests that recrystallization occurs by formation and growth of spherulites. The transition from blocky to spherulitic elongated grain morphology occurs more quickly at higher temperature. Figures 1C and 1D show blocky grains after a 1050°C/1 sec RTP anneal and elongated grains after a 1050°C/2 sec treatment. We find that similar microstructures develop in stoichiometric Y-123 fibers at about 25°C higher temperaturesl.

Both the blocky- and elongated-grain microstructures consist primarily of orthorhombic Y-123. This is confirmed by TEM of crushed fragments of fibers. Figure 2 is a bright field TEM of a fragment of a stoichiometric Y-123 fiber after an RTP anneal at 1025°C for 1 sec. The obvious twins indicate that the material is orthorhombic Y-123, a fact confirmed by electron diffraction.

Rapid Oxygenation

Green Y-123 fibers sintered by RTP are superconducting with zero resistance near 90K immediately after the rapid anneal [1]. We have also observed that Y-123 fibers pretreated with a conventional (eg., 925°C/30 min.) air sintering anneal to produce dense, largely tetragonal semiconducting fibers, can be rendered superconducting by RTP, suggesting that ultra-rapid oxygenation occurs in RTP. To investigate the rapid oxygenation effect, we prepared a series of stoichiometric Y-123 fibers by sintering fibers 30 minutes at 945°C in an atmosphere of flowing nitrogen. These N_2-sintered samples were semiconducting before RTP, but became superconducting after RTP treatment at 1000°C.

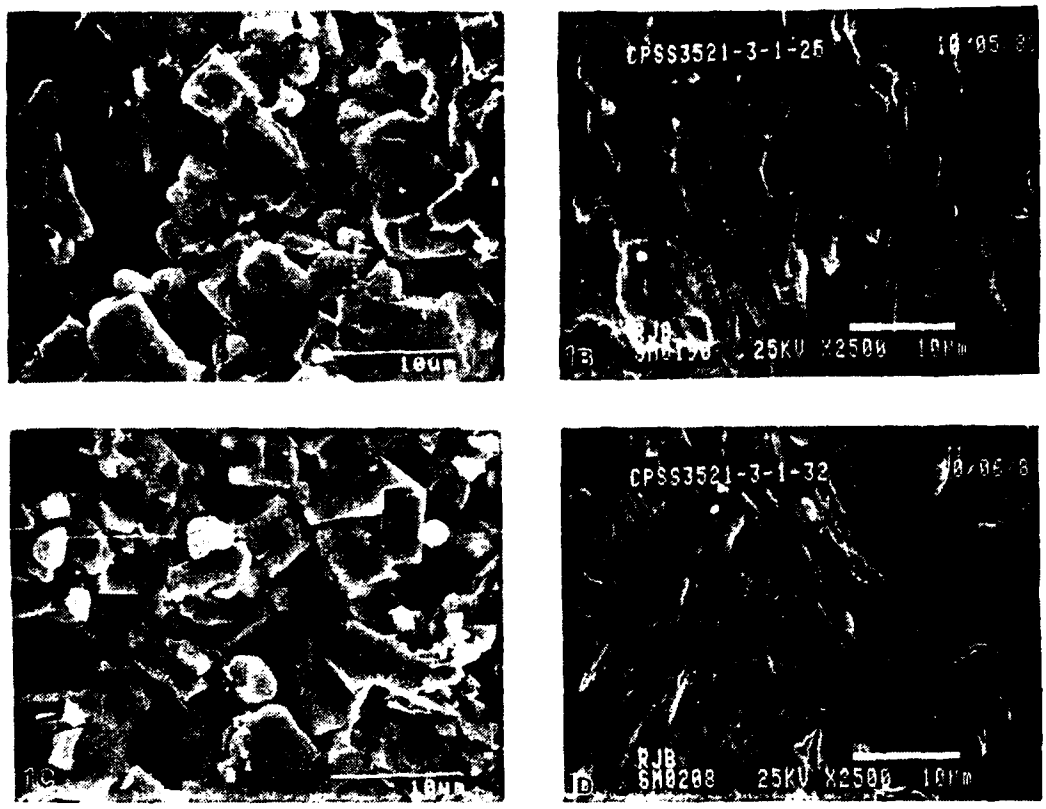

Figure 1 SEM Micrographs showing grain morphology in unsintered Y-123 + 5 wt% CuO wires, after RTP anneals of: A) 1025°C, 2 sec; B) 1025°C, 4 sec; C) 1050°C, 1 sec; D) 1050°C, 2 sec

Figure 2 Transmission electron micrograph of twinned orthorhombic Y-123 from a stoichiometric Y-123 wire sintered by RTP at 1025°C

Figure 3, a plot of resistivity vs. temperature, illustrates that the N_2-sintered fibers had a resistivity above 2000 $\mu\Omega$-cm, with no hint of a resistive transition. A 1-second RTP treatment reduces the normal state resistivity below 300 $\mu\Omega$-cm, with a partial transition near 90K. After a 2-second RTP treatment, the specimen displays a broad transition with onset at 87K and zero resistance at 78K. The 4-second RTP treatment sharpens the transition, so that onset occurs at 92K with zero resistance at 87K.

Figure 4 shows the real and imaginary volume AC susceptibility down to 75K for the N_2-presintered fibers after 1000°C/1 sec RTP. No diamagnetism could be detected at 77K with this technique in the as-sintered specimen. The 2-second RTP sample has a small diamagnetic signal, reaching only -0.05 at 77K, while the 4-second sample has a diamagnetic susceptibility as high as -0.40 at 77K.

Table I displays the SQUID data for volume static susceptibility (diamagnetic shielding) in 100 Oe at 5K. Like other ceramic Y-123 samples, these RTP fibers have weak-link behavior, so in a 100 Oe field the grains are decoupled, allowing volume susceptibility to be estimated from the measured mass susceptibility. Completely superconducting grains would have a volume static susceptibility of $-1/4\pi$. We assume that the 5K data can be used as a rough indication of the extent of oxygenation of the Y-123. A more quantitative estimate would require corrections for the magnetic penetration depth and grain morphology. At 5K, the N_2 sintered sample had a measurable diamagnetic susceptibility, demonstrating that small fraction of orthorhombic phase exists after N_2 sintering. The susceptibilities of the 1000°C RTP samples cooled at the standard rate of 4°C/sec were similar when the dwell time was varied from 1 seconds to 4 seconds, indicating that little further oxygenation occurs after the first second. The peak temperature of the RTP treatment seems to be important, since heating to 850°C reduced the 5K susceptibility.

It runs counter to intuition to suggest that 1-4 second dwells at peak temperature causes oxygenation, since the equilibrium oxygen content at 1000°C is known to be in the non-superconducting tetragonal range. A more likely explanation would seem to be that the material oxygenates during the rapid cool. To test this, a series was run with constant dwell time, but cooling rates either twice as fast (8°C/sec) or twice as slow (2°C/sec) than the standard rate. This would have a decisive affect if the reoxygenation occurred during the rapid cool. The data of Table I, however, show that the volume susceptibility is not affected by the cooling rate. Thus we reach the surprising conclusion that RTP increases the oxygen stoichiometry at 1000° to levels high enough to create orthorhombic 90K material. The mechanism for this is unclear.

Transmission electron microscopy of the N_2 sintered Y-123 before RTP shows that most of the grains are tetragonal. A few grains are partially converted to orthorhombic, often with twins growing inward from the grain boundaries. This is consistent with partial reoxygenation by O^2 impurities, and is the origin of the small diamagnetic signal at 5K. Figure 5 is a series of bright field images from ion-milled foils. Figure 5A shows one of the more partially orthorhombic grains in the as-sintered material. The twins are poorly developed and a large number of (as yet uncharacterized) lattice defects are visible. The twins boundaries are not crisply defined, an indication of oxygen depletion. The 1000°C-1 sec. RTP reduces the population of tetragonal grains and improves the quality of the orthorhombic grains. Figure 5B shows "cleaner" twin boundaries and fewer lattice defects. After the 1000°C-2 sec. RTP, most of the microstructure is similar to Figure 5C, with minimal defects and the sharp twin boundaries which are a sign of high oxygen content.

Summary

Rapid thermal processing, involving 2-4 sec. around 1000°C with a 3 min. cool down in oxygen, forms the dense sintered fibers of orthorhombic Y-123. Green fibers are rapidly densified, displaying microstructures characterized by large grains with distinctive blocky or elongated morphology. Presintered Y-123 fibers do not undergo drastic microstructural change after RTP, but are

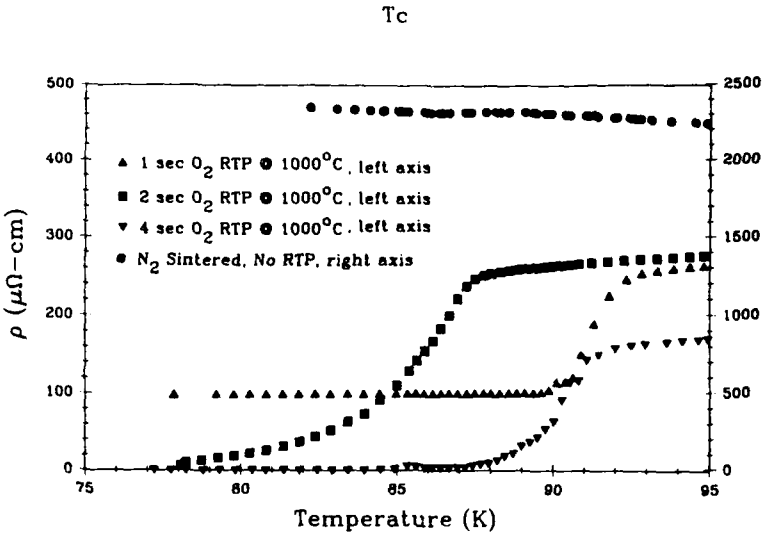

Figure 3 Resistivity vs. temperature for stoichiometric Y-123 fibers pre-sintered in nitrogen and RTP annealed in oxygen at 1000°C

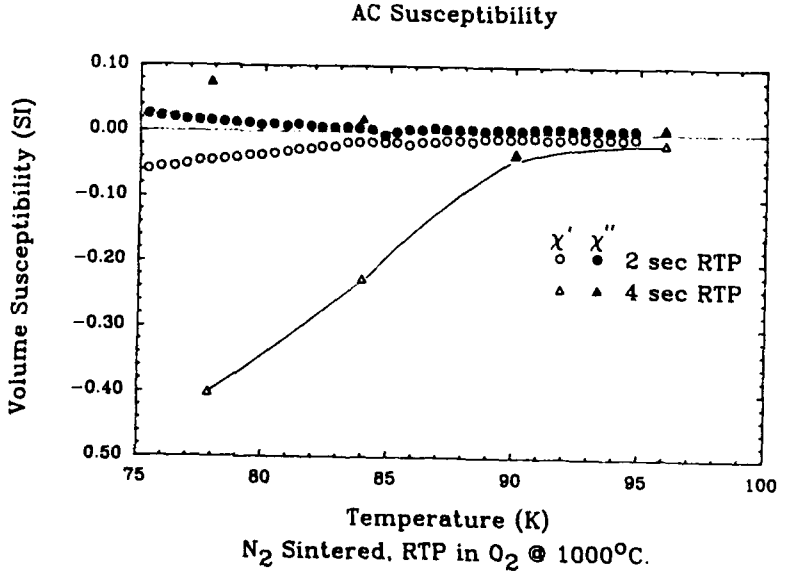

Figure 4 Real and imaginary AC susceptibility for stoichiometric Y-123 fibers pre-sintered in nitrogen and RTP annealed in oxygen at 1000°C

TABLE I

DIAMAGNETIC SHIELDING DATA AT 5K FOR NITROGEN-SINTERED Y-123

RTP PROCESS CONDITIONS	VOLUME SUSCEPTIBILITY AT 100 Oe
AS- SINTERED, NO RTP	-0.10/4π
1000°C - 2 sec hold - 2°C/sec cool	-0.21/4π
1000°C - 2 sec hold - 4°C/sec cool	-0.23/4π
1000°C - 2 sec hold - 8°C/sec cool	-0.24/4π
1000°C - 1 sec hold - 4°C/sec cool	-0.25/4π
1000°C - 4 sec hold - 4°C/sec cool	-0.26/4π
850°C - 2 sec hold - 4°C/sec cool	-0.15/4π

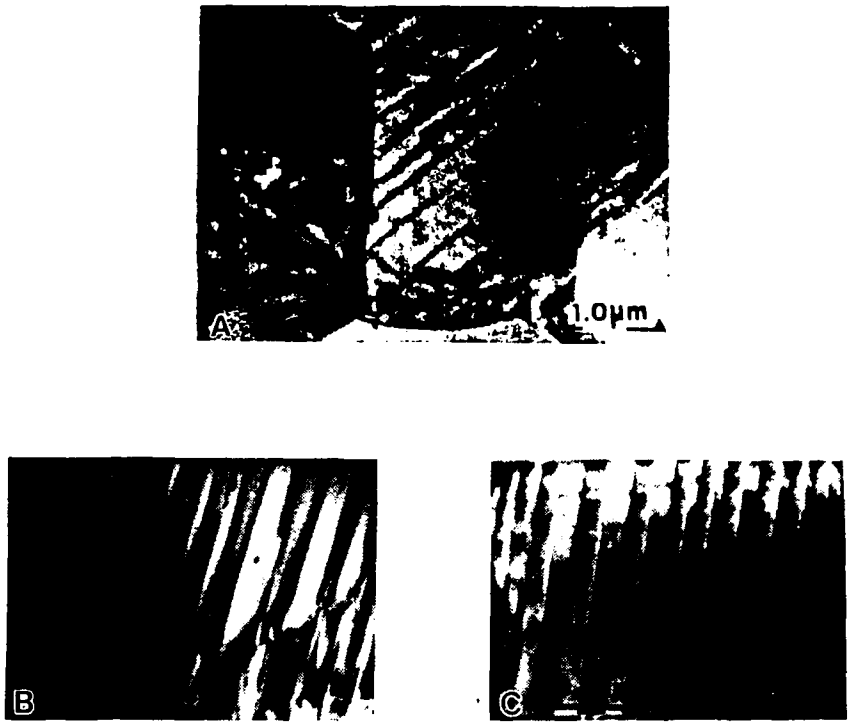

Figure 5 Bright field transmission electron micrographs of the nitrogen sintered series: A) as-sintered state, no RTP; (B) 1000°C/1 sec RTP; (C) 1000°C/2 sec RTP

rapidly oxygenated by the treatment. Presintered fibers, semiconducting and tetragonal before RTP, form twinned orthorhombic material after RTP with T_c to 90K and magnetization indicative of substantially shielding.

Experiments with RTP of tetragonal Y-123 fibers made by pre-sintering in N_2 show that re-oxygenation by RTP in oxygen occurs during the 1-4 second isothermal hold at 1000°C, rather than during the 3-minute cooling ramp. Twinned orthorhombic Y-123 grows predominantly from grain boundaries, suggesting grain boundary diffusion of oxygen during the RTP anneal.

Acknowledgements

The work at CPS Superconductor was supported by DARPA contract N00014-88-C-0512 and NASA-Lewis contract NAS-3-25876. The Los Alamos work was supported by the High Temperature Superconductor Pilot Center Cooperative Agreement CRDA-89-03. The work at Sandia was supported, in part, by the DOE Office of Basic Energy Sciences under contract No.DE-AC04-76DP00789.

References

1. D.S. Ginley, E.L. Venturini, J.F. Kwak, M. Mitchell, R. J. Baughman, J.W. Halloran, and M.J. Neal, Physics Review Letters (in press 1990)

2. D.S. Ginley, E.L. Venturini, J.F. Kwak, R. J. Baughman, R.J. Bourcier, M.A. Mitchell, B. Morosin, J.W. Halloran, M.J. Neal, and D.W. Capone, in High Temperature Superconductors: Fundamentals, Properties, and Novel Processing, ed. J. Narayan et al. Materials Research Society, Symposia Proceedings Volume 196 , (in press 1990)

ATTACHMENT I

REPORT SUMMARY

COMPOSITE CERAMIC SUPERCONDUCTING WIRES FOR ELECTRIC MOTOR APPLICATIONS

Seventh Quarterly Report on
Contract Number N00014-88-C-0512

April 30, 1990

John W. Halloran, Ceramics Process Systems Corporation,
Milford, MA 01757

This report describes progress on developing Y-123 wire for an HTSC motor. The HTSC homopolar motor is being fabricated. HTSC wire for the field coils has been produced, and the process is being scaled-up to fabricate the coils. Silver clad polycrystalline Y-123 wire is being sintered with a continuous process. Development began on post-processing of sintered Y-123 wire by directional crystallization. In parallel development, green fiber, green clad wire, and sintered polycrystalline wire has been fabricated from the BiSCCO material. The sintered BiSCCO wire can be cold rolled into a tape.

After installing an extension to the sintering furnace, a process is in place in which spools of green clad fiber are fed into the belt furnace and collected as spools of sintered clad wire at the furnace exit. We have made steady progress toward continuous uninterrupted furnace operation. We are developing annealing procedures for long wires, which will be batch annealed as coils of sintered wire.

Melt texturing research work is underway at CPS exploring a range of YBCO compositions and Ag-Pd coatings. Preliminary experiments have been done in preparation for the upcoming subcontracts at A.D. Little and Oak Ridge National Laboratory aimed at melt processing of wires and fibers. Also, work continued in collaboration with Sandia and Los Alamos National Laboratories on rapid thermal processing of Y-123, with most emphasis on characterizing the rapid oxygenation effect.

The design of the HTSC homopolar motor has been improved to increase the output from field coils by using six smaller coils, each with separately optimized current. Motor construction is in progress. Preliminary design is underway on a DC heteropolar motor with HTSC field windings and armature and a brushless "trapped flux permanent magnet" DC motor, in which the field is produced by trapped flux in an HTSC rotor.

ATTACHMENT II

ARPA ORDER NUMBER: 9525

PROGRAM CODE NUMBER: 7737

CONTRACTOR: Ceramics Process Systems Corporation
155 Fortune Boulevard
Milford, MA 01757

CONTRACT NUMBER: N00014-88-C-0512

CONTRACT EFFECTIVE DATE: 30 JUNE 1988

CONTRACT EXPIRATION DATE: 31 MARCH 1991

SHORT TITLE OF WORK: High Temperature Superconducting Wire and Motor

PRINCIPAL INVESTIGATOR: John W. Halloran
(508) 634-3422

This report describes progress on developing Y-123 wire for an HTSC motor. The HTSC homopolar motor is being fabricated. HTSC wire for the field coils has been produced, and the process is being scaled-up to fabricate the coils. Silver clad polycrystalline Y-123 wire is being sintered with a continuous process. Development began on post-processing of sintered Y-123 wire by directional crystallization. Sintered polycrystalline wire also has been fabricated from the BiSCCO material. The sintered BiSCCO wire can be cold rolled into a tape.

After installing an extension to the sintering furnace, a process is in place in which spools of green clad fiber are fed into the belt furnace and collected as spools of sintered clad wire at the furnace exit. We are developing oxygen annealing procedures for long wires as coils.

Melt texturing research work is underway at CPS with preliminary experiments done at A.D. Little and Oak Ridge National Laboratory aimed at melt processing of wires and fibers.

The design of the HTSC homopolar motor has been improved to increase the output from field coils. Motor construction is in progress. Preliminary design is underway on a DC heteropolar motor with HTSC field windings and armature and a brushless "trapped flux permanent magnet" DC motor.

ATTACHMENT III

ARPA ORDER NUMBER: 9525 PROGRAM CODE NUMBER: 7737

CONTRACTOR: Ceramic Process Systems Corporation
155 Fortune Boulevard
Milford, MA 01757

CONTRACT NUMBER: N00014-88-C-0512 CONTRACT AMOUNT: $ 5,509,387.00

EFFECTIVE DATE OF CONTRACT: 30 JUNE 1988

EXPIRATION DATE OF CONTRACT: 31 MARCH 1991

PRINCIPAL INVESTIGATOR: John W. Halloran

TELEPHONE NUMBER: (508) 634-3422

SHORT TITLE OF WORK: High Temperature Superconducting Wire and Motor

REPORTING PERIOD: 1 January 1990 through 31 March 1990

DESCRIPTION OF PROGRESS

This report describes progress on producing Y-123 wire for an HTSC motor. Wire development emphasized production and scale-up of continuously sintered wire, resulting in the production of a spool of sintered silver clad wire 166 meters long. The wire is being sintered with a continuous process in which spools of green clad fiber are fed into the belt furnace and collected as spools of sintered clad wire at the furnace exit. We have made steady progress toward continuous uninterrupted furnace operation, with the longest run lasting 13 hours before a wire break. We are developing a method to batch annealed long wires in a coiled state. In parallel development of BiSCCO wire, green fiber, green clad wire, and sintered polycrystalline wire has been fabricated from the BiSCCO material. The sintered BiSCCO wire can be cold rolled into a tape.

Development began on post-processing of sintered Y-123 wire by directional crystallization. Melt texturing research work is underway at CPS exploring a range of YBCO compositions and Ag-Pd coatings. Preliminary experiments have been done in preparation for the upcoming subcontracts at A.D. Little and Oak Ridge National Laboratory aimed at melt processing of wires and fibers by floating zone methods and a novel technique of metal jacketed zone melting. Collaborative research continue with Sandia and Los Alamo National Laboratories on rapid thermal processing of Y-123, with most emphasis on characterizing the rapid oxygenation effect.

The design of the HTSC homopolar motor has been improved to increase the output from field coils by using six smaller coils, each with separately optimized current. Motor construction is in progress. Preliminary design is underway on a DC heteropolar motor with HTSC field windings and armature and a brushless "trapped flux permanent magnet" DC motor, in which the field is produced by trapped flux in an HTSC rotor.

SUMMARY OF SUBSTANTIVE INFORMATION DERIVED FROM SPECIAL EVENTS

Project members attended the several conferences on high temperature superconductivity to keep abreast of current developments.

CHANGE IN KEY PERSONNEL

No change

PROBLEMS ENCOUNTERED AND/OR ANTICIPATED

None

ACTION REQUIRED BY THE GOVERNMENT

None

FISCAL STATUS (March 31, 1990)

1) CUMULATIVE AMOUNT CURRENTLY RECEIVED ON CONTRACT . . . . . $ 2,976,264

2) CUMULATIVE EXPENDITURES AND COMMITTMENTS TO DATE..... $ 3,129,189

3) ADDITIONAL FUNDS REQUIRED TO COMPLETE WORK[1]

THROUGH FY 1990..... $ 1,077,811

[1] According to a revised spending plan formulated with Dr. Frank Patten on March 28, 1990